PALAIOS
Emphasizing the impact of life on Earth's history

PALAIOS, 2008, v. 23, p. 667–682
Research Article
DOI: 10.2110/palo.2007.p07-016r

TAPHONOMIC FEATURES OF *PALEODICTYON* AND OTHER GRAPHOGLYPTID TRACE FOSSILS IN OLIGO-MIOCENE THIN-BEDDED TURBIDITES, NORTHERN APENNINES, ITALY

PAOLO MONACO
Dipartimento di Scienze della Terra, Università degli Studi di Perugia, Piazza dell'Università 1-06100 Perugia, Italy
e-mail: pmonaco@unipg.it

ABSTRACT

Taphonomic features of 156 graphoglyptids and other trace fossils preserved as hypichnia of thin-bedded turbidites in Oligo-Miocene flysch of the northern Apennines (central Italy) were analyzed. Two biogenic taphonomic categories—deformation and elongation—were produced in hemipelagic mud by the behavior of endobenthic organisms. Deformation includes such features typical of bulldozing and burrowing as twisting, squeezing, tilting, thickening, and widening. Elongation is considered a primary biogenic character controlled directly by the tracemaker. Taphonomic features induced by such physical agents as currents and creep usually developed unidirectionally and include stretching, straightening, smoothing, bending, tapering, thickening, and thinning. These features, associated with hundreds of microgrooves (5–10 per 0.01 m^2) interpreted as mud-current lineations, suggest that currents were active and produced deformational structures of fluting before, during, and after the biogenic activity. Preservation of such delicate structures recognizable at different levels is particularly noticeable when a thin layer of fine material settled by suspension, molding all structures and producing a cemented film. Deformational structures may be particularly well preserved in thin-bedded (3–6-cm-thick) and fine-grained calcarenitic turbidites as in diluted turbulent flow deposits that fringed the isolated Verghereto High. Activities of epi- and infaunal communities in this area are also exceptionally well preserved. Physical taphocharacters of graphoglyptids are interpreted in two ways: (1) as true tool marks produced in mud by a tractive water mass preceding sand deposition by turbidite flows, or (2) as structures inherited from preturbidite phases. Taphonomic analysis in deep-sea deposits, therefore, is a promising methodology to resolve the preservational state of trace fossils above and below the soles of turbidites.

INTRODUCTION

Taphonomic features of 156 trace fossils preserved as hypichnia of thin-bedded turbidites in Oligo-Miocene flysch deposits of the northern Apennines foredeep basins, central Italy, were analyzed (Fig. 1). Variations in the shape of the geometric patterns of burrows are taphonomic characteristics that conform to methods used by Bromley (1996), Monaco (2000), and Monaco and Giannetti (2002). Such parameters as elongation, deformation, and thickening or thinning that affect shafts, meshes, ramous meanders, and strings that define ichnotaxa provide new data to improve the preservation models of Seilacher (1977b; 2007) and Crimes and Crossley (1980). Moreover, taphonomic observations presented here provide a better characterization of the role played by currents and biogenic activity in the preservation of hypichnia at soles of turbidite deposits.

Paleodictyon Menghini, 1850, is a distinct trace fossil preserved commonly as casts on the sole of fine- to medium-grained turbidites (Peruzzi, 1881). It is a three-dimensional burrow system composed of a regular, repetitive net made up of horizontally distributed hexagonal meshes and vertical outlets to the seafloor. *Paleodictyon* belongs to the group of trace fossils known as graphoglyptids (Fuchs, 1895), which includes a large number of ichnotaxa (Książkiewicz, 1970, 1977; Seilacher, 1977a; 1977b; 2007). Seilacher (1977b) postulated several behavioral programs including nutritional strategies in food-restricted, deep-sea environments. Burrowing strategies are still unsolved and the nature of many of the tracemakers remains unknown (Miller, 1991; Wetzel, 2000; Uchman, 2004). Some studies refer to these trace fossils as solitary burrowers, colonial protists (xenophyophorans?), or other types of organisms (Swinbanks, 1982; Levin, 1994; Rona et al., 2003; Rona, 2004). A mathematical analysis of *Paleodictyon* patterns raises questions about whether it should be considered a burrow and whether it was constructed by a single organism or by multiple organisms (Honeycutt and Plotnick, 2005). Tracemakers of *Paleodictyon* are inferred to be farming microbes and are, therefore, included in the ethologic group of agrichnia (Ekdale, 1985). *Paleodictyon* was constructed in many environments during the early Paleozoic (Orr, 2001) and have been found in deep-water turbidite deposits from the Late Cretaceous to Paleogene (Fuchs, 1895; Seilacher, 1962, 1974, 1977b; Uchman, 1995a, 1998, 2004; Wetzel, 2000). Seilacher (1977b, fig. 1, p. 292) proposed that *Paleodictyon* and other forms of graphoglyptids were produced in mud that was eroded and cast by sand-rich turbidites; these burrows are referred to as predepositional trace fossils (Książkiewicz, 1954; Seilacher 1962). The preservation of graphoglyptids as turbidite sole casts, therefore, depends strictly on the erosion of the seafloor in front of a turbidity current and the time of casting (Seilacher, 1974; Uchman, 1995a; Tunis and Uchman, 1996a, 1996b).

Crimes and Crossley (1980) noted that *Paleodictyon* provides much information about bottom currents. For example, the long axes of hexagonal meshes are not always parallel to the sole marks of the turbidite; they deviate by a few degrees (Crimes and Crossley, 1980; table 1). This suggests that the preferential orientation of the long axis reflects the orientation of bottom currents in between episodes of turbidite deposition. Elongation and their parallel orientation to the main current flow may have facilitated the convergence of current flows through all the tunnels of the burrow system (Crimes and Crossley, 1980, fig. 5). The role of the seafloor consistency and the displacement of the sediment in a slope environment—downslope gravity creep—remain unresolved. Crimes and Crossley (1980) suggested that *Paleodictyon* could be used to infer the direction of the paleocurrent and to define changes in flow directions near distal facies.

Few studies have been made on the taphonomic features of *Paleodictyon* and other deep-water graphoglyptids, even though the preservation potential of taphonomic alterations induced by physical or biogenic processes may be detectable at the soles of fine-grained turbidites (Seilacher, 2007). In order to test the models introduced by Seilacher (1977b; 2007) and Crimes and Crossley (1980), the taphonomic characteristics of ichnocoenoses preserved as hypichnia of turbidites in Oligo-Miocene flysch of the Northern Apennines were analyzed. This allowed the physical and biogenic processes to be quantified and the role of erosion and casting in deep-sea deposits to be appraised.

 0883-1351/08/0023-0667/$3.00

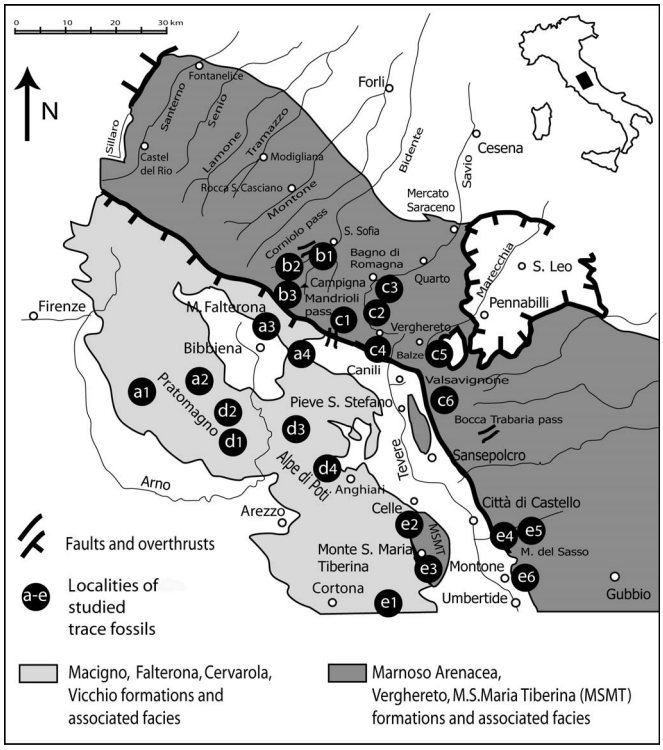

FIGURE 1—Locality map and flysch deposits containing *Paleodictyon*, graphoglyptids, and other trace fossils. Letters inside circles indicate main outcrops reported in Table 1.

GEOLOGICAL SETTING

Oligo-Miocene siliciclastic turbidites of the northern Apennines, central Italy, analyzed here are the Macigno, Falterona, Cervarola, Vicchio, Marnoso Arenacea, Verghereto and M. S. Maria Tiberina formations (Fig. 1). The Macigno, Falterona, Cervarola and Vicchio formations (Tuscan successions, Oligocene-early Miocene) are found mainly in southern Romagna and central to southern Tuscany, whereas the Marnoso Arenacea, Verghereto and M. S. Maria Tiberina formations (autochthonous successions, early to late Miocene) developed mainly in the eastern- and southernmost sector of Tuscany (e.g., south of Tiber valley, Fig.1), northern and central Umbria and southern Romagna (Ricci-Lucchi, 1981; Boccaletti and Coli, 1982; Abbate and Bruni, 1989; Boccaletti et al., 1990; Costa et al., 1997; Plesi et al., 2002). They were formed in foredeep and piggy back basins thrusted and folded toward the northeast and filled with siliciclastic deposits. These deposits produced deep-sea fan systems within a basin-plain setting composed of depositional lobes, fringing facies, and thick muds on isolated submarine highs (e.g., the Verghereto High). Such environments do not fit the classic deep-sea, fan-basin-plain model due to the extreme morphological complexity and irregularity of the Apennine foredeep seafloor.

Oligo-Miocene flysch deposits are thin- to thick-bedded and consist of fine- to coarse-grained arenites and calcarenites, 3–250 cm thick, intercalated with gray to darkgray hemipelagic mudstones, 30–350 cm thick. Pebbly mudstone and slump deposits are also associated commonly with these deposits. Bioturbation in thinner beds is widespread and represented mainly by hypichnia and epichnia, whereas trace fossils in thicker beds are hypichnia or endichnia (mainly *Scolicia strozzii*) and vertical multilayer colonizers (e.g., *Ophiomorpha* and *Thalassinoides*), which cross two or three beds vertically or obliquely (Uchman, 1995a; 2007; Monaco et al., 2007). Sandstones and calcarenites are thinly layered. Mica flakes, dark pebbles, and black plant detritus are very abundant and are selectively concentrated in the laminae. These laminae consist of graded, plain-parallel (dominant) traction carpets and wavy, cross-laminated, climbing to symmetrical, rippled sandy to silty deposits (very common northwest of Verghereto). Convoluted and water-escape structures are also common.

Thick-bedded turbidites—mainly coarse-grained sandy facies (F4–F6) of the turbidite model of Mutti (1992)—are typical of the Macigno and Falterona formations and crop out mainly in the Pratomagno Ridge (Table 1). They are interpreted as structureless, gravelly to sandy, high-density turbidite current-flow deposits. Graphoglyptids in thick-bedded turbidites are very poorly preserved because of abundant tabular scours and large grooves (up to 60 cm wide). These facies are important when trying to understand the compaction history of these units because the cross-sectional shape of the tunnels in such endichnia as *Chondrites*, *Ophiomorpha*, and *Thalassinoides* varies from circular to elliptical in shape. For example, *O. rudis* often have oblique cross grooves, flute casts, and frondescent marks at the soles of thick-bedded turbidites. Thick-bedded turbidites are probably depositional lobes, which make up the most common type of sandstone bodies in the basin fill of the northern Apennine foredeep and correspond to the maximum extent to which the NW–SE-oriented sand bodies were transported into the basin (Walker, 1984; Mutti and Normark, 1987; Mutti, 1992)

Medium-bedded turbidites are assigned mainly to facies F7–F8, whereas thin-bedded turbidites are assigned to facies F9, low-density turbidite currents (LDTC), or thin-bedded deposits (Table 1). Facies F7 is characterized by thin, horizontal laminae that likely represent traction carpets. Several thin traction-carpet layers can be found from the base to the top in the same 30–50-cm-thick bed and may be only a few grains thick (Mutti, 1992, plate 42A–B). Facies F8 is considered a true Ta Bouma division and consists of structureless, medium- to fine-grained sandstone.

Thin-bedded turbidites (fine-grained facies F9) typically characterize distal areas of outer fans or fan-fringe facies of lobes and basin plain; graphoglyptids are very abundant and well preserved in these facies. Facies F9 can be subdivided into facies F9a and F9b. According to Mutti (1992), facies F9a is commonly a Ta-missing turbidite bed, showing the typical incomplete Tb–e or Td–e type sequence of the Bouma sequence. Facies F9b has a higher sand/mud ratio than facies F9a, is internally less organized, composed of slightly coarser sediments than very fine grained sandstone, and is characterized by ripple bedforms. Deposits of the F9b facies probably indicate a high fall-out rate from a suspension current (e.g., Mutti, 1992, p. 74). Small-sized specimens of *Paleodictyon strozzii*, *P. majus*, *P. italicum*, *P. minimum*, *Paleodictyon* isp., and other graphoglyptids are very abundant at the soles of the F9a and F9b facies, where taphonomic features are also well preserved. Large-sized *P. hexagonum* specimens, usually found in facies F9a, may be partially scoured (Montone and Campigna localities, see Table 1).

In the Verghereto High, the muddy facies are very thick (up to 400 m) and contain sporadic thin-bedded turbidites (F9b facies, 3–5 cm thick, Montecoronaro in Table 1). Turbidite bodies tend to become progressively thicker towards the north; this suggests a gradational transition from the F9a–b facies to the northwest of the Verghereto High to the F7–F8 facies of the Bagno di Romagna depositional fan. In the Verghereto High, the top of thin-bedded deposits is rippled and shows such meandering or sinuous trace fossils as *Nereites missouriensis* and *Scolicia prisca*. Small ripples suggest varying directions in weak bottom currents (Piper and Stow, 1991; Mutti, 1992). Other thin-bedded, fine-grained turbidites show the turbidite mud sequence T0–T8–P and E1–E3–F (Stow and Piper, 1984a, 1984b; Walker, 1984). Some graphoglyptids have been found (e.g., *Urohelminthoida*), but the top of the bed, which is the hemipelagite-pelagite transition (T8-P or E-F, respectively, see Monaco and Uchman, 1999; Wetzel and Uchman, 2001), is poorly bioturbated (e.g., *Chondrites*).

ICHNOLOGY

Rich graphoglyptid ichnocoenoses made up of many ichnotaxa are summarized in Table 2. Only 156 trace fossils catalogued in the ICHNOTHECA of the Biosedimentary Laboratory at the Earth Science Department of the University of Perugia show interesting taphonomic features for analysis. *Paleodictyon* is the most useful for taphonomic analysis. Sixty-three *Paleodictyon* specimens studied belong to *P.*

TABLE 1—Studied outcrops.

Locality No. (see Fig. 1)	Coordinates (UTM/WGS 84)	Geological map (1:100.000)	Formations	Studied turbidites	Facies (Mutti, 1992)
Pratomagno ridge					
a1 Poggio Regina	434010 005230	No. 107 Falterona	Macigno, Falterona	thick to medium beds	F4-F8
a2 Cetica	434120 004730	No. 107 Falterona	Macigno, Falterona	thick to medium beds	F4-F8
M. Falterona area					
a3 Pratale	434620 004010	No. 107 Falterona	Cervarola, Vicchio	medium to thin beds	F9a-b
a4 C. d. Verna area (N)	434350 003130	No. 107 Falterona	Cervarola, Vicchio	medium to thin beds	F9a-b
Corniolo Pass					
b1 Corniolo	435430 004030	No. 107 Falterona	Marnoso Arenacea, Verghereto	thin beds	F9a-b
La Calla and Mandrioli Passes; upper Savio and Tiber river valley, from Bagno di Romagna to south of Verghereto High					
b2 Campigna (NE)	435350 004120	No. 107 Falterona	Marnoso Arenacea, Verghereto	thin beds	F9a-b
b3 Campigna	435250 004230	No. 107 Falterona	Marnoso Arenacea, Verghereto	thin beds	F9a-b
c1 Cantoniera Mandrioli	434830 003110	No. 107 Falterona	Marnoso Arenacea, Verghereto	thin beds	F9a-b
c2 Savio South	434820 002830	No. 108 Mercato Saraceno	Marnoso Arenacea, Verghereto	thin beds	F9a-b
c3 Savio North	434940 002930	No. 108 Mercato Saraceno	Marnoso Arenacea, Verghereto	thin beds	F9a-b
c4 Canili	434530 003510	No. 108 Mercato Saraceno	Marnoso Arenacea, Verghereto	thin beds	F9a-b
c5 Montecoronaro	434650 002510	No. 108 Mercato Saraceno	Marnoso Arenacea, Verghereto	thin beds	F9a-b
c6 Valsavignone	434410 002520	No. 108 Mercato Saraceno	Marnoso Arenacea, Verghereto	thin beds	F9a-b
Southern part of Pratomagno ridge, Alpe di Poti-Catenaia (Ar)					
d1 Poggio la Cesta	433550 004430	No. 114 Arezzo	Macigno, Falterona	mainly thick beds	F4-F6
d2 S. Maria Carda	433850 004140	No. 114 Arezzo	Falterona, Cervarola	thick to medium beds	F7-F8-F9a
d3 Monte Filetto	433540 003040	No. 114 Arezzo	Falterona, Cervarola	medium to thin beds	F8-F9a-b
d4 Quarantola (Poti)	432920 003050	No. 114 Arezzo	Falterona, Cervarola	medium to thin beds	F8-F9a-b
Cortona (Ar), Monte S. Maria Tiberina area, Soara river valley, Montone					
e1 Montanare	431450 002050	No. 122 Perugia	Falterona, Cervarola	medium to thin beds	F8-F9a-b
e2 Celle area (NW)	432850 001630	No. 115 Città di Castello	Vicchio	medium to thin beds	F8-F9a-b
e3 Monte S. Maria Tiberina	432530 001620	No. 115 Città di Castello	M.S.M. Tiberina	medium to thin beds	F8-F9a-b
e4 M. del Sasso	432650 000930	No. 115 Città di Castello	Marnoso Arenacea	medium to thin beds	F8-F9a-b
e5 Soara valley	432730 000820	No. 115 Città di Castello	Marnoso Arenacea	medium to thin beds	F8-F9a-b
e6 Montone	432220 000530	No. 115 Città di Castello	Marnoso Arenacea	medium to thin beds	F8-F9a-b

hexagonum (17 specimens, 12 were *Glenodictyum*, and 5 *Ramodictyon*, *sensu* Seilacher, 1977b), *P. strozzii* (2 specimens), *P. majus* (6 specimens), *P. italicum* (6 specimens), *P. minimum* (11 specimens), *P. latum* (5 specimens), *Paleodictyon* isp. (13 specimens) and *Squamodictyon* (3 specimens) (Table 2).

The ichnotaxonomy of *Paleodictyon* is based mainly on the geometry of the nets (regular or irregular), the maximum mesh size, the ratio of the maximum mesh size (MMS) to the string diameter (SD), and the preservation of vertical shafts with or without mesh (Sacco, 1888; Vialov and Golev, 1965; Seilacher, 1977b; Uchman, 1995a). Seilacher (1977b) proposed such subichnogeneric names for *Paleodictyon* as: (1) *Glenodictyum* to indicate only horizontal hexagonal meshes, (2) *Ramodictyon* when vertical shafts are preserved, and (3) *Squamodictyon* to indicate scalelike meshes. Recently, Uchman (1995a) redefined the morphometric range of *Paleodictyon* in flysch deposits using the maximum mesh size and string diameters, distinguishing 13 species, including very small (*P. minimum* and *P. latum* with MMS values of 0.1–0.3 mm and SD values of 0.2–0.9 mm) and very large forms (*P. italicum*, *P. hexagonum* and *P. gomezi* with MMS >10 mm and SD >2.5 mm). In this classification, it is often difficult to distinguish between the two forms of the *Ramodictyon* subichnogenus, *R. tripatens* and *R. nodosum* (Seilacher, 1977b), because each *Glenodictyum* specimen may also be preserved as *Ramodictyon* when vertical shafts are preserved. *R. nodosum* and *R. tripatens*, therefore, should be used with caution. In this study, specimens of *Glenodictyum* were considered apart from *Ramodictyon* (Table 3). The first consists of a large net, 80 cm wide and 120 cm long, with SD of 2.8–4 mm and a MMS of $\sim$14 mm (Table 3). Vertical shafts and knobs (knob diameter $=$ 6–8 mm and knob length $=$ 10–12 mm; Table 3) are located at three branching points of the mesh, such as in *R. tripatens* (Seilacher, 1977b, fig. 14g). Mesh widening or elongation may have affected the string diameter, thereby influencing the taxonomic affinity; specimens with a very wide, widened string (Uchman, 1995a) are also known as *P. robustum* (Koriba and Miki, 1939).

The remaining ichnotaxa considered in this study include both graphoglyptid and nongraphoglyptid specimens and are subdivided into knob-shaped (38 specimens), ramous-shaped (39 specimens), and string-shaped or meandering trace fossils (16 specimens) (Tables 2–3). In general, knob-shaped and ramous-shaped forms are taxonomically meaningful only when they are geometrically distributed or follow closely spaced meanders at soles of fine-grained turbidites; they also cross *Paleodictyon minimum* meshes. Trace fossils can be indicated as generic plug-shaped structures when preservation is poor and taxonomic determination is doubtful (Table 3). The main knob-shaped or radiate ichnotaxa recognized in the studied material include: *Lorenzinia* isp. (9 specimens), *Parahaentzschelinia* isp. (7 specimens), *Helicolithus ramosus* (3 specimens), and *Bergaueria* isp. (4 specimens). Other ramous-shaped (uni- and biramous) graphoglyptids include *Desmograpton* (20 specimens), *Paleomeandron* (4 specimens), *Urohelminthoida* (10 specimens), and *Protopaleodictyon* (3 specimens). The meandering and string-shaped trace fossils are *Cosmorhaphe* (2 specimens), *Helminthorhaphe* (3 specimens), *Spongeliomorpha* (4 specimens), and *Protovirgularia* (8 specimens) (see Tables 2–3). *Ophiomorpha rudis* and *Scolicia strozzii*, although very abundant, were not considered in this study.

TABLE 2—Description of ichnogenera.

Ichnogenus	Short description
Paleodictyon Meneghini, 1850	Hypichnial mesh of hexagons and shafts. For extended description, see text. 63 specimens.
Lorenzinia Gabelli, 1900	Radial structure with short, smooth, hypichnal ridges arranged in one or two circular rows radiating from round central area; *Lorenzinia pustulosa*, *Lorenzinia plana*, and *Lorenzinia* isp. have been found. 9 specimens.
Parahaentzschelinia Chamberlain, 1971	Hypichnial circular to oval knobs, up to 20 mm in diameter of vertical shafts, radiating subvertically from one master shaft. 7 specimens.
Helicolithus Azpeitia Moros, 1933	Series of regular and parallel knobs, 0.3–1 mm in diameter, up to 100 per dm^2 and regularly spaced in sole of fine-grained turbidites; studied specimens of *Helicolithus ramosus* very similar to *Punctorhaphe parallela*. 3 specimens.
Bergaueria Prantl, 1945	Vertical plug-shaped trace fossil, circular to elliptical in cross section with rounded base and apical depression with essentially structureless sandy fill; specimens of *Bergaueria* cf. *hemispherica* as hypychnial mounds 15–25 mm long and 15–17 mm high, oval in outline, at lower surface of fine-grained, silty turbidites. 4 specimens.
Cosmorhaphe Fuchs, 1895	Meandering graphoglyptid with two orders of regular and widely spaced meanders; in *C. lobata* second-order undulations are better preserved than first-order ones and usually of greater wave length than amplitude. In *C. parva* regular, second-order undulations are slightly higher than wide. 2 specimens.
Desmograpton Fuchs, 1895	Hypichnial trace fossil formed by double rows of string-sized, J- or U-shaped, semimeanders joined by bars. Curved segments inwardly oriented in alternating position; rare are two opposite semimeanders joined by short bars. In 5 specimens of *Desmograpton ichthyforme*, bars narrowly aligned and appear as parallel and very long ridges; perpendicular bars seldom preserved. In 15 specimens of *Desmograpton dertonensis*, narrow U-shaped semi-meanders occur. 1 specimen of *Desmograpton* cf. *alternum* displays alternate semi-meanders elevated in curved positions. 21 specimens.
Paleomeandron Peruzzi, 1881	Meandering string preserved as hypichnia with rectangular second-order meanders. *P. transversum* shows first-order, widely spaced meanders and sharp turning points marked by cross bars; *P. robustum* exhibits pairs of thin knobs, 0.2–0.4 mm wide, distributed inside meanders, which probably represent vertical shafts; *P. elegans* with second-order undulations and sharp corners and *Paleomeandron* isp. have been found. 4 specimens.
Urohelminthoida Sacco, 1888	Hypichnial string-sized, tight meanders, in which turning points are angular, and regularly spaced appendages protrude outwardly from turning points. *U. dertonensis* is more common and typical and commonly forms regular meanders, 30–45 mm wide, and shows hypichnial strings up to 4 mm in diameter; appendages are up 60 mm long. *U.* cf. *appendiculata* exhibits slightly irregular meanders, which are tight (distance two or three times tunnel diameter) and very wide, with a course becoming convex; appendages short, parallel to tunnels. 10 specimens.
Helminthorhaphe Seilacher, 1977	Nonbranching hypichnial trace fossil of variable string diameter (up to 4 mm in *H.* cf. *japonica*) with one order of smooth meanders. In *H. japonica*, specimen from Cervarola Formation meanders show very high amplitude. 3 specimens.
Protopaleodictyon Książkiewicz, 1958	Hypichnial wide first-order meanders, more or less regular in shape, with short appendages branching from apex of second-order meanders. Three specimens of *Protopaleodictyon minutum* and *Protopaleodictyon* isp. from sole of fine-grained turbidites exhibit interesting taphonomic features. 3 specimens.
Plug-shaped structures (undetermined)	Circular to elliptical, essentially structureless sandy filled structures, 1 to 3.5 mm in diameter, randomly distributed in groups as hypichnia at soles of thin-bedded turbidites. 15 specimens.
Spongeliomorpha de Saporta, 1887	Simple, string-shaped horizontal burrow usually with set of longitudinal or obliquely disposed, fine and elongate striations on exterior. Usually this predepositional trace produces a displacement of mud current lineations and other trace fossils. Main ichnospecies is *S. sublumbricoides* with ridges and striae disposed obliquely and grouped. 4 specimens.
Protovirgularia McCoy, 1850	Horizontal, cylindrical trace fossil, distinctly or indistinctly bilobate, straight or slightly meandering. Characteristics are internal structures, formed by successive pads of sediment disposed at both sides, expressed on exterior as typical ribs arranged in chevronlike biserial pattern (*P. oblitera-ta*). *Protovirgularia vegans* usually undulate in vertical plane (semi-lune) and therefore preserved as hypichnial disrupted ridges with close flute casts. 8 specimens.

TAPHONOMY

Taphonomic analysis of trace fossils (Figs. 2–3) focused on the morphologic deviations from the original shapes caused by biogenic or physical agents (Bromley, 1990, 1996; Fernández López, 1997; Monaco, 2000; Monaco and Giannetti, 2002; Caracuel et al., 2005; Savrda, 2007). In large and small ichnotaxa of *Paleodictyon*, superimposed meshes of the same ichnospecies are found: two for *Paleodictyon hexagonum* and two for *P. minimum*; they always have a peculiar arrangement and are arranged as superimposed rows of cells (see 2Msh in Fig. 2G). The shallow upper parts of the shafts and deep mesh levels are commonly separated by a difference in height (step in Figs. 3A–C). This step varies from 10–30 mm for large *Paleodictyon* specimens (*P. hexagonum*) to 2–3 mm for small specimens (*P. minimum*). It highlights two orders of erosional processes that affect the seafloor at different depths and involve one or more meshes and vertical shafts (Figs. 3A–C). In *Paleodictyon minimum* both mesh levels are exposed: a deep one, 2–4 mm below the paleosurface, and a shallow one closer to the sediment-water interface (dpm and shm, respectively, in Fig. 3C). In all small examples of *P. minimum* at Quarantola (Alpe di Poti, see Tables 1–3), the number of processes that affect meshes decreases from the deepest (dpm) to the shallowest level (shm). Two taphonomic characteristics that only affect the shallow mesh are indicated in Figure 3C.

Taphonomic characteristics can be attributed to biogenic and physical agents: the former produced three-dimensional deformations, whereas the latter produced unidirectional deformations on both the mesh plane and shafts (Fig. 4). Twelve taphonomic features that involve deep and shallow mesh, knobs, and ramous meanders are listed below; their abbreviations are summarized in Table 3. Outlines of biogenically and physically induced features are summarized in Figure 4. In many samples these features are often associated.

Taphonomic Features Induced by Biogenic Agents

Two separate groups of biogenically induced taphonomic features can be recognized: (1) three-dimensional deformations and (2) elongation. Unlike elongation, which is directly controlled by the tracemaker, three-dimensional (3-D) deformations can be considered to be a byproduct of burrowing. This kind of secondary deformation can occur in five different ways, depicted in Figure 4, and briefly described below.

Twisting.—Twisting can be considered a 3-D deformation because it develops along the x-y-z axes (Fig. 4). A portion of trace fossil (e.g., one

TABLE 3—Taphonomic features of 156 specimens. Taxonomy symbols: MMS = maximum mesh size; SD = string diameter; SL = string length; MW = meander width; KnL = knob length; KnDm = knob diameter; KnDs = knob distance. Taphonomy symbols: Tws = twisting; Sqz = squeezing; Tlt = tilting; Tck = thickening; Wdn = widening; Elg = elongation; Str = stretching; Stg = straightening; Smo = smoothing; Bnd = bending; Tpr = tapering; Thn = thinning.

Ichnotaxa	No.	Biosedlab samples	Category	Aspect	Level	Taxonomy	Taphonomy	Agents
Paleodictyon (*Glenodictyum*) *hexagonum*	9	MA13, 18, 28, 57, 115, 118, 145, 160, 179	net shaped	horizontal mesh (deep)	1 of 2	MMS >10mm; SD >2.5mm	Tws; Sqz; Tlt; Tck; Wdn; Elg (deep m.)	Biogenic
Paleodictyon (*Glenodictyum*) *hexagonum*	3	MA14, 57, 140	net shaped	horizontal mesh (medium)	1 of 2	MMS >10mm; SD >2.5mm	Str; Stg; Smo (medium mesh)	Physical (currents, creeping)
Paleodictyon (*Ramodictyon*) *hexagonum*	5	MA13, 14, 28, 145, 189	knob shaped	vertical outlets	1	KnDm 6–8mm; KnDs 10–12mm	Stg; Bnd; Tpr; Thn	Physical (current flow)
Paleodictyon strozzii	2	MA101a–b	net shaped	horizontal mesh	1	MMS >2<6mm; SD >0,2<1mm	Str; Smo	Physical (current flow)
Paleodictyon majus	6	MA117, 182, CEV148, PT129a–c	net shaped	horizontal mesh	1	MMS >5<12mm; SD >0.8<15mm	Str; Smo; Wdn	Physical (current flow)
Paleodictyon italicum	6	MA32, 202, 183, 208a–c	net shaped	horizontal mesh	1	MMS >20<40mm; SD >2.8mm	Tws; Str	Physical; biogenic
Paleodictyon latum	5	MA211a–e	net shaped	horizontal mesh (shallow)	1 of 2	MMS >0.1<0.3mm; SD >0.4<0.9mm	Str; Stg; Smo (shallow mesh)	Biogenic; physical (current flow)
Paleodictyon minimum	11	MA211a–j	net shaped	horizontal mesh (deep)	1 of 2	MMS >0.1<0.3mm; SD >0.2<0.3mm	Elg; Wdn (deep mesh)	Biogenic
Paleodictyon (*Glenodictyum*)	12	MA67, 200, 212a–i	net shaped	horizontal mesh	1	MMS >30<40mm; SD >1<2mm	Tws; Str; Smo	Biogenic; physical
Paleodictyon (*Ramodictyon*)	1	MA29	knob shaped	vertical outlets	1	KnDm 2–3mm; KnDs 7–12mm	Stg; Tpr; Thn; Smo	Physical (current flow)
Paleodictyon (*Squamodictyon*)	3	MA102, 164, 213	net shaped	horizontal mesh	1–2?	MMS >2.5<3.5mm; SD >2.5<4mm	Tws; Tck; Wdn; Str	Physical; biogenic
Lorenzinia plana	5	MA 61, 108; 169; 173, 213	knob shaped	radial	1	KnL >2.5<4mm	Smo; Stg; Bnd; Tpr; Thn	Physical (current flow)
Lorenzinia pustulosa	1	PT141a	knob shaped	radial	1	KnL >2<6mm	Tck	Biogenic; physical?
Lorenzinia isp.	3	PT141b–d	knob shaped	radial	1	KnL >2<5mm	Stg; Bnd; Tpr; Thn	Physical (current flow)
Parahaentzschelinia isp.	7	MA90, 92, 165, 174a–d	knob shaped	group	1	KnL >3<6mm	Smo; Stg; Bnd; Tpr; Thn	Physical (current flow)
Helicolithus ramosus	3	MA58.188,192	knob shaped	scattered	1	KnL >0.2<0.6mm	Smo; Stg	Physical (current flow)
Bergaueria cf. *hemispherica*	4	MA23a–d	knob shaped	single	1	KnL >15<25mm	Smo	Physical (current flow)
Plug-shaped structures	15	MA213a–q	knob shaped	scattered	1	KnL >5<14mm	Tck; Tlt; Smo	Biogenic; physical
Cosmorhaphe lobata	1	PT 126	meandering	wide meanders	1	SD >3<5mm; MW >40<60mm	Sqz; Thn; Tck; Smo	Biogenic; physical
Cosmorhaphe parva	1	MA 105	meandering	narrow meanders	1	SD >2<5mm; MW >2<5mm	Tck; Smo	Biogenic; physical
Desmograpton ichthyforme	4	MA25, 81, 93, 94	ramous shaped	biramous, straight string	1	SD >0.8<2mm; SL >2<14mm	Stg; Smo; Tck; Thn	Physical (current flow)
Desmograpton dertonensis	16	MA36, 88, 168, 175, 184, 186, 190, 205, 212a–g	ramous shaped	biramous, straight string	1	SD >0.8<2mm; SL >2<14mm	Stg; Smo; Tck; Thn; Tws; Sqz	Physical; biogenic
Desmograpton cf. *alternum*	1	MA36	ramous shaped	biramous, straight string	1	SD >0.8<1.8mm; SL >0.9<4mm	Stg; Smo; Tck; Thn	Physical (current flow)
Paleomeandron transversum	1	MA192	ramous shaped	biramous, curved string	1	SD >2<4mm; SL >2<6mm	Smo; Thn	Physical (current flow)
Paleomeandron elegans	1	CEV53	ramous shaped	biramous, curved string	1	SD >1.8<2.2mm; MW >3<4.5mm	Smo; Thn	Physical (current flow)
Paleomeandron robustum	1	CEV178	ramous shaped	biramous, curved string	1	SD >2<8mm; MW >12<16mm	Smo; Thn	Physical (current flow)
Paleomeandron isp.	1	MA213f	ramous shaped	biramous, curved string	1	SD >1<4mm; MW >10<12mm	Smo; Thn	Physical (current flow)
Urohelminthoida dertonensis	4	MA27, 37, 54, 191	ramous shaped	uniramous, tightly meander	1	SD >2<5mm; MW >35<60mm	Stg; Smo; Tck; Thn	Physical (current flow)
Urohelminthoida isp.	5	MA60, 62, 68, 69, 122	ramous shaped	uniramous, tightly meander	1	SD >2<4mm; MW >35<60mm	Stg; Smo; Tck; Thn	Physical (current flow)
Urohelminthoida appendiculata	1	MA64	ramous shaped	uniramous, tightly meander	1	SD >1.2<2mm; MW >20<60mm	Smo; Tck; Thn	Physical (current flow)
Helminthorhaphe isp.	1	CEV48	meandering	tightly meander	1	SD >1.3<2mm; MW >60<80mm	Smo; Tck; Thn	Physical (current flow)
Helminthorhaphe japonica	2	MA199a, CEV199b	meandering	tightly meander	1	SD >1.2<2mm; MW >40<70mm	Smo; Thn	Physical (current flow)
Protopaleodictyon minutum	2	MA35, 203	ramous shaped	winding meander	1	SD >2<3.5mm; MW >30<60mm	Stg; Smo; Tck; Thn	Physical (current flow)

TABLE 3—Continued.

Ichnotaxa	No.	Biosedlab samples	Category	Aspect	Level	Taxonomy	Taphonomy	Agents
Protopaleodictyon isp.	1	MA61	ramous shaped	winding meander	1	SD >1<2mm; MW >20<40mm	Smo; Tck; Thn	Physical (current flow)
Spongeliomorpha isp.	4	MA234a–c, 196	string shaped	straight string	—	SD >8<25mm; SL >50<250mm	Tlt; Tws; Tck; Sqz	Biogenic (head)
Protovirgularia obliterata	5	MA15, 87, 197, 201, CEV 159	string shaped	straight string	—	SD >1<7mm; SL >10<220mm	Smo; Tck; Tlt (others P)	Physical; biogenic
Protovirgularia vagans	2	MA44, 116	string shaped	meandering string	—	SD >5<20mm; SL >100<320mm	Smo; Tck	Physical (current flow)
Protovirgularia ? isp.	1	MA234d	string shaped	meandering string	—	SD >5<20mm; SL >100<320mm	Smo; Bnd	Biogenic (mainly)

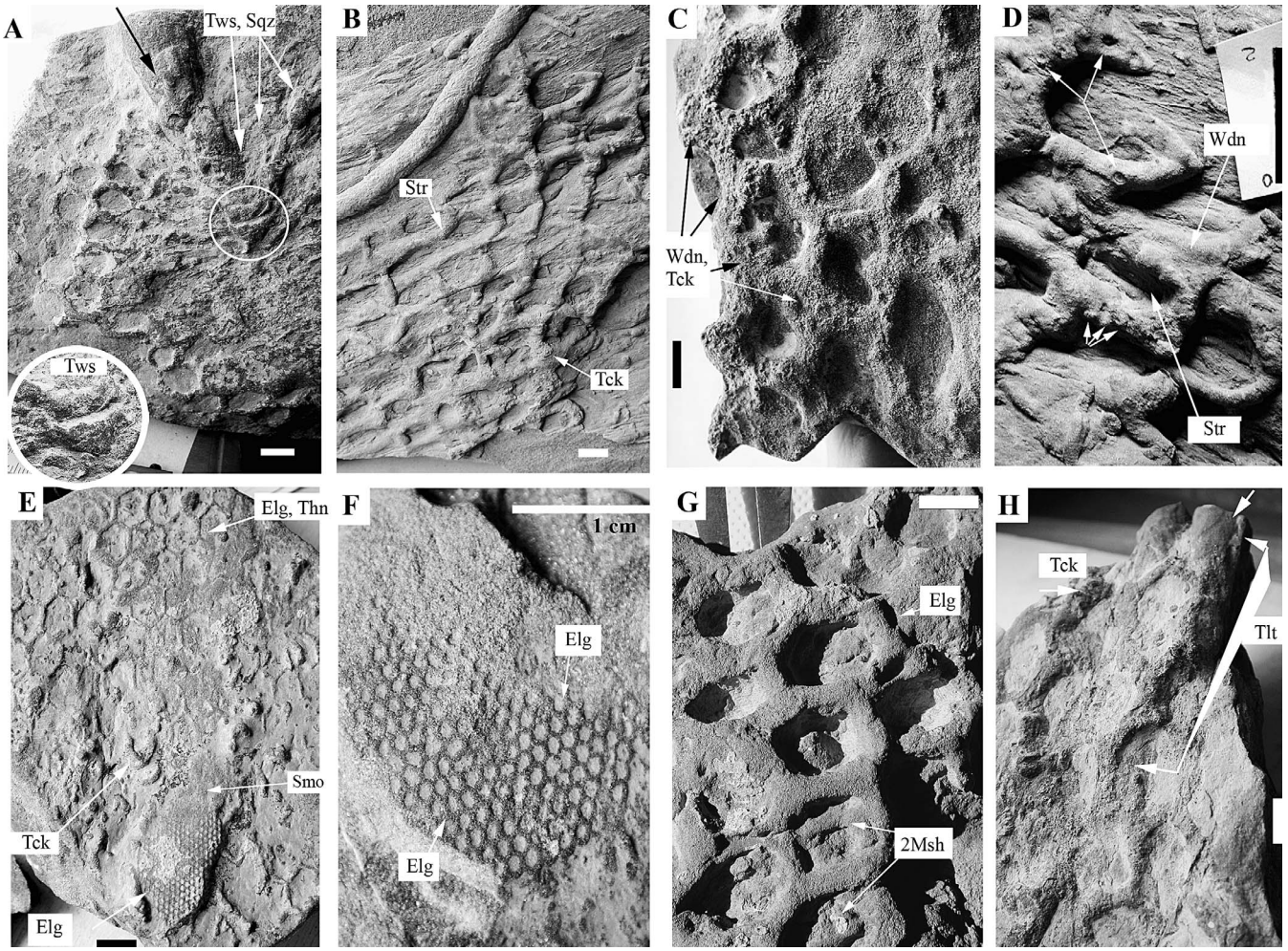

FIGURE 2—Biogenic taphonomic features affecting mesh of large to small *Paleodictyon* specimens preserved as hypichnia at soles of thin-bedded turbidites, Marnoso Arenacea and other formations, northern Apennines, Oligocene-Miocene. Scale bar is 1 cm for all samples. A) *P.* (*Glenodictyum*) *hexagonum* mesh with biogenic squeezing (Sqz) and twisting (Tws; see circle) by bulldozer activity (arrow); sample MA18, Verghereto NW. B) Mesh of *P.* (*Glenodictyum*) *hexagonum* with thickening (Tck) and cells crossed by tubular burrows. Physical unidirectional stretching (Str) is present and major axis lengths of hexagons triple; sample MA57, Canili of Verghereto. C) Microspots in mesh walls of *P.* (*Glenodictyum*) *hexagonum* induced by microburrowing to produce thickening (Tck) and widening (Wdn); sample MA140, Città di Castello (M. del Sasso locality). D) Detail of B showing widening (Wdn) and stretching (Str) of cells and branching points; note holes and circles (upper white arrows) and miniknobs (lower white arrows). E) Elongation (Elg) associated with thinning (Thn) in *Paleodictyon* isp., *P. minimum* (below) and *P. majus* (top); thickening (Tck) produces horseshoe shape; sample MA211a, Alpe di Poti (Arezzo area). F) Elongation (Elg) involves net meshes in small-sized *P. latum* with two preferred orientations (arrows); sample MA211b, Alpe di Poti (Arezzo area). G) Two net levels (2Msh) characterize large *P. hexagonum*; the deep one is elongated (Elg), sample MA28, Città di Castello (north of Monte S. Maria Tiberina). H) Burrowing activity (tubular intrusion, see arrow) induces tilting (Tlt) and thickening (Tck) of *P. hexagonum* mesh; sample CEV179, Mandrioli Pass.

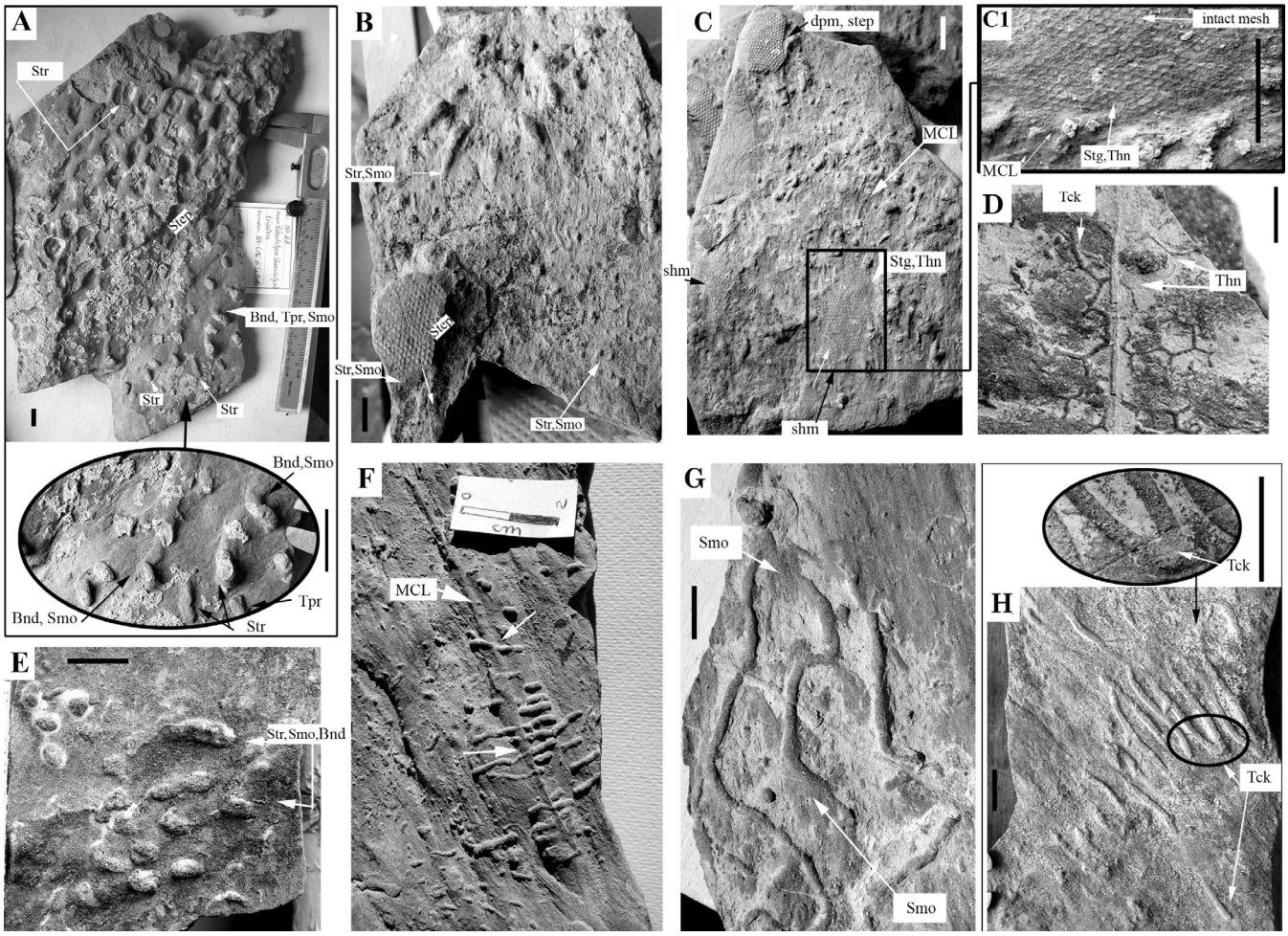

FIGURE 3—Physical taphonomic features caused by currents affecting meshes, shafts, knob- and meander-shaped traces preserved as hypichnia at soles of thin-bedded turbidites, Marnoso Arenacea and other formations, northern Apennines, Oligocene-Miocene. Scale bar is 1 cm for all samples. A) Bending (Bnd), tapering (Tpr), and smoothing (Smo) of the shallow level where shafts of *Paleodictyon* (*Ramodictyon*) *hexagonum* developed (arrows in the oval); note 50°–60° angles from stretching (Str) of shafts and that of mesh and the step between the two levels; sample MA28, Città di Castello (north of Monte S. Maria Tiberina). B) Radiating elements of knob-shaped *Lorenzinia* (top), deep mesh (lower left), and shallow outlets (lower right) of *P. minimum* subject to stretching (Str) and smoothing (Smo) induced by interturbidite bottom currents; note preservation of delicate structures and the step; sample MA211c, Alpe di Poti (Arezzo area). C) Deep (dpm, upper left) and shallow (shm, lower left and center) meshes of *P. minimum*; note thinning (Thn) and straightening (Stg) of shallow mesh where hexagons are parallel and oriented in the direction of the main current flow, suggested by microgrooves (mud-current lineations, MCL); sample MA211d, Alpe di Poti (Arezzo area); in detail of C1 note the intact mesh at top and straightening (Stg) and thinning (Thn) in the lower part at the end of MCL. D) String diameter of hexagons in partially preserved mesh of *P. majus* subject to thinning (Thn) and thickening (Tck); sample MA101, Verghereto NW. E) Knob-shaped *Parahaentzschelinia* isp. with stretching (Str) and smoothing (Smo); sample MA90, Verghereto Balze. F) *Desmograpton dertonensis* cross a minigroove induced by a preturbidite current (MCL upper arrow), note undisturbed tunnels (arrows); sample MA36, Verghereto NW. G) Smoothing (Smo) affects one side of *Helminthorhaphe* cf. *japonica* tunnels; note small mud-current lineations in upper part of sample, MA199, Mandrioli Pass. H) Thickening (Tck) of string-shaped semimeander of *D. ichthyforme* (arrows); note detail of thickening (Tck) in the oval; sample MA25, Verghereto Balze.

or more cells) can be twisted around an axis rotating up to 80° and the trace fossil can also be slightly translated from its original position (Fig. 4). In large specimens of *Paleodictyon hexagonum*, twisting has been observed in a lump of contiguous cells (Figs. 2A, 5). A sample of *Desmograpton dertonensis* shows opposite meanders that are slightly twisted and displaced by the intrusion of a burrower in the mud (e.g., predepositional *Protovirgularia*).

Squeezing.—Although squeezing may develop together with twisting (e.g., in a specimen of large *Paleodictyon hexagonum*), it can be considered separately among the other taphonomic characteristics because it is an exclusively horizontal deformation (Fig. 4). Squeezing is easy to establish when it develops along the same plane. In this case, hexagonal meshes partially or totally change in shape; cells become closer, with an overall width reduction of 70% (Fig. 2A). Squeezing is difficult to quantify in meander- or knob-shaped trace fossils, although it has been observed in *Desmograpton dertonensis* and *Cosmorhaphe lobata* specimens.

Tilting.—Tilting is deformation that uplifts the whole plane of the mesh, pivoting on one side and tends to rise progressively from its original position; a slight translation can also be observed. In many specimens of large *Paleodictyon*, tilting was produced by the intrusion of a burrower below the mesh level; the push of the intruder indirectly deformed many hexagons of the mesh (Fig. 2H). Tilting, as in the case of squeezing, was considered separately among the deformational characteristics because it linearly and progressively affects some rows of hexagons (Fig. 4).

Thickening.—This characteristic is also observed in part of the hexagons of the net of large *Paleodictyon* specimens; it may also be associated with such characteristics as squeezing and twisting. Thickening was produced by the subsequent deformation of both contiguous cells and branching points in mesh-shaped trace fossils (Fig. 2B, 4). Thickened strings—their diameter commonly doubles, reaching 6 mm—usually develop oriented transversally to the stretching direction (Fig. 2D). When longitudinal segments or hexagon vertices are thickened, they contain many mini-knobs, and the tunnels are irregularly distributed (see white and black arrows, respectively in Fig. 2C). In two samples, dark grains

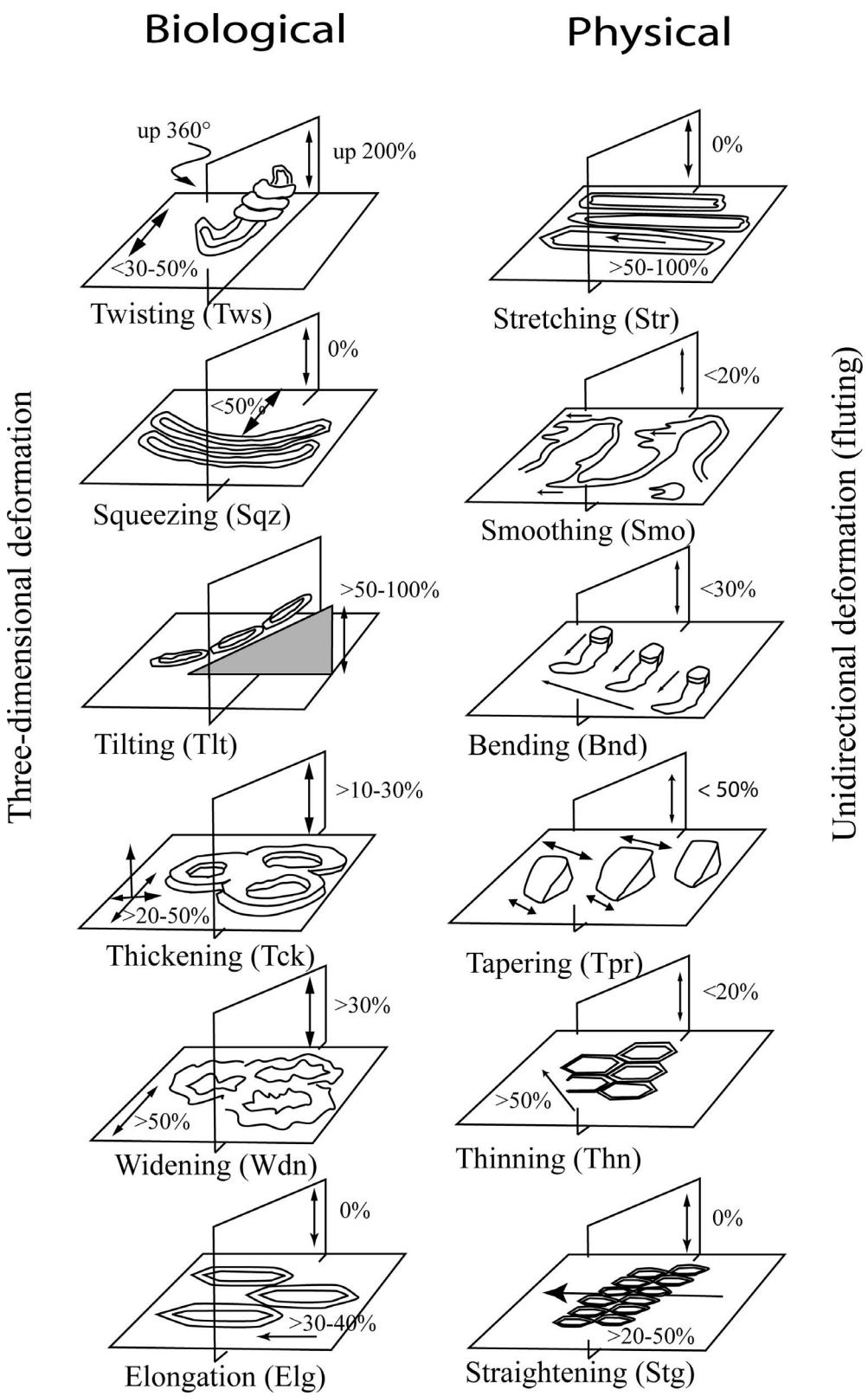

FIGURE 4—Taphonomic features (six biogenic and six physical). See text for explanation.

and rounded, coarse quartz crystals were densely packed. Thickened fillings were often burrowed, and many smaller diameter trace fossils were also present (meiofauna?, see holes and circles of 1–2 mm indicated by three upper white arrows in Fig. 2D).

Widening.—Although not very common, this feature is also associated with thickening. It may be found at branching points in large *Paleodictyon* but is observed also in other string parts. When the biogenic activity of subsequent burrowing was intense, some parts were thickened, whereas others were widened. Thickening, however, caused an omnidirectional expansion of strings (vertically and laterally), whereas widening produced

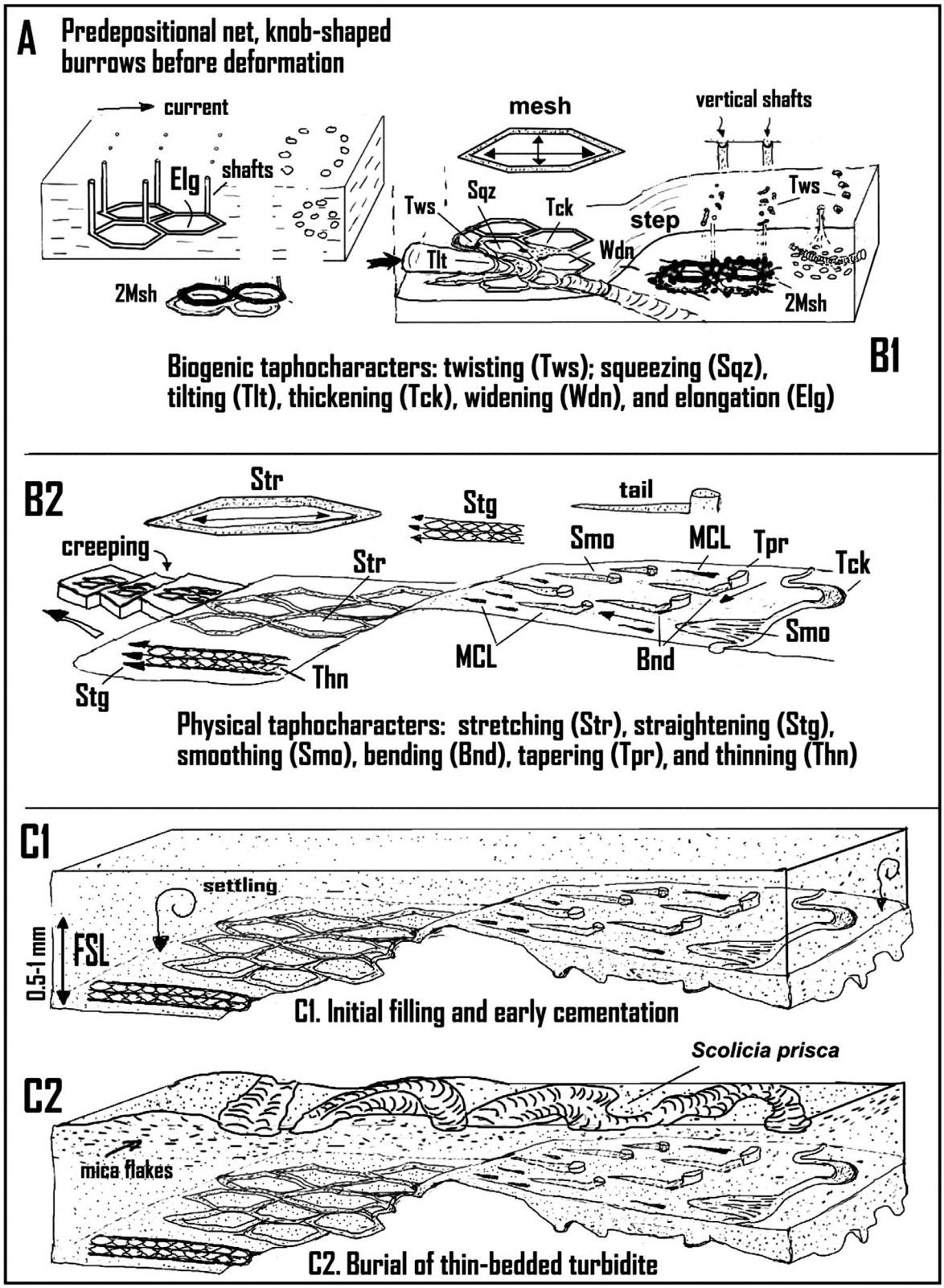

FIGURE 5—A synthetic model to explain taphonomic characteristics of hypichnial *Paleodictyon* specimens and other graphoglyptids and epichnial trace fossils. (A) Predepositional burrowing. (B) Biostratinomic features (B1 biogenic and B2 physical) affecting meshes, shafts, knobs, and ramous meanders. (C) Final stage, initial filling and burial of turbidite sand. Fine spread level (FSL) is a 0.5–1.0-mm-thick level, which preserves all taphonomic features of graphoglyptids and mud-current lineations (MCL).

a reduction in thickness (vertical flattening) with a lateral expansion of hexagons; in many graphoglyptid specimens, expanded branching points are directly contiguous to thickened hyporeliefs (Figs. 2C–D, 4). Mini-knobs are abundant in widened parts of tunnels (see Fig. 2D). Mini- and micro-knob concentrations suggest that microbioturbation was intense in branching points in which the concentration of the organic matter (and bacteria ?) were abundant; see very small, externally oriented knobs indicated by three lower white arrows in Figure 2D. In very rare instances compaction flattened the entire mesh; this has been observed in both strings and all branching points of small- to medium-sized *Paleodictyon*. A similar aspect is the compactional collapse of burrows in mud described in turbidite deposits (cf. Seilacher, 1977b, fig. 1f).

The bulldozer activity induced by mud-stirring burrowers is the major cause of twisting, squeezing, tilting, thickening, and widening**.** This is especially clear when effects of intrusion in mud are recognizable along the x-y-z axes. In many cases, hexagons were squeezed or twisted and thickened or widened, and their shape tends to change from hexagonal to rectangular or irregular (Figs. 2A–B in the center). In other instances meshes may be tilted up vertically, 2–3 cm from their original level, and both their diameter and original shape are preserved (Fig. 2H). Twisting, squeezing, and tilting are usually more developed near the point of maximum pressure (i.e., the point of bulldozing intrusion, Figs. 2A, H); the mesh is tightly arranged with curved festoons around the source of intrusion. This suggests that the mud was stiff but still plastic (Ekdale, 1985). In other cases, microbioturbation produced a considerable increase in the volume or in the diameter (e.g., thickened and widened points). Microbioturbation may be present also in bulldozing-induced deformations and it may emphasize other taphonomic features.

Elongation.—This feature is deformation directly controlled by the tracemaker. It involves the lengthening of hexagons approximately in the same direction; variation in the length of each hexagon is the same for the entire mesh. This phenomenon is very interesting in *Paleodictyon minimum*, *P. latum*, and *P. majus* (Figs. 2E, 4). In the deep mesh of *P. minimum* and *P. latum*, the delicate rows of hexagonal cells are elongated in the same direction (Figs. 2E–F). The maximum mesh size has two different axes (minor axis of 0.1 mm, major axis of 0.3 mm, respectively; Fig. 2F), whereas the string diameter (mean value 0.2 mm) in the deep mesh does not vary. Analysis of hundreds of cells has shown that the elongation value was the same in all 11 specimens. The living organism(s) may have controlled elongation in small *Paleodictyon* specimens during the (late?) burrowing phase as suggested by Crimes and Crossley (1980). This characteristic does not appear to be a typical biostratinomic feature *sensu stricto.* The major axis of the hexagons may elongate parallel to the current indicators and maximize the passive ventilation of the open burrow system (Crimes and Crossley, 1980). In small *Paleodictyon* as well as in many other graphoglyptids, therefore, current should be the most important factor that influences the size and shape of the burrows. Other biological factors have also been suggested for such deformation (Seilacher, 1977a; Bromley, 1996; Wetzel, 2000). Elongation was observed in two ichnospecies in the same sample (e.g., *Paleodictyon majus* with *P. strozzii*, or *P. minimum* with *P. majus*) (Fig. 2E); in these cases, the organisms that produced these traces interacted in a small space in order to exploit physical irrigation by currents (commensal relationships, see Ray and Aller, 1985; Bromley, 1990).

Taphonomic Features Induced by Physical Agents

In the studied specimens, deformation attributable to physical factors acts unidirectionally (Fig. 4) and was produced by such physical agents as the current action before or after burrowing. Fluting can be considered the main cause of physically induced features. Physical deformation results in many taphonomic byproducts affecting predepositional hypichnial trace fossils (Fig. 4).

Smoothing.—Smoothing (Smo) is a typical feature in many samples that resulted from a fluting process that caused partial destruction of the down-current side of tunnels and produced a broad, apron-shaped structure or tail (Figs. 4, 6E). These structures, 3–40 mm long, that form an angle of 45–90° with the string development, were very abundant (>20 in one sample) and were probably produced in soft mud by selectively altering the shape of the burrows (Fig. 3G). They are analogous to the fluted half reliefs described by Seilacher (1977b) and Crimes and Crossley (1980). Smoothing has been mainly reported in meander-shaped *Helminthorhaphe* and ramous-shaped *Desmograpton* and *Urohelminthoida*, but it has also been observed in knob-shaped shafts of large *Paleodictyon* specimens (Fig. 3A) and in the plug-shaped trace fossil *Bergaueria*, *Lorenzinia*, and *Parahaentzschelinia*.

Bending.—Bending (Bnd) is one of the typical effects of fluting and suggests the existence of currents with different directions. Bending and smoothing are frequently associated in the same sample, but their orientations are different. This association of bending and smoothing as products of unidirectional currents leads to the exclusion of compaction as the primary factor. Bending is also present when knobs are not compacted. It has been found in the shafts of large *P.* (*Ramodictyon*) *hexagonum*, and has also been observed in such plug-shaped forms as *Parahaentzschelinia*, where typical bent segments of the down-current tail have been observed. The bending ranges from 30° to 80°, and tends to give the trace fossil a hooked appearance (Figs. 3A, details enlarged in oval; 6E).

Stretching.—Stretching (Str), as a typical effect of fluting, differs substantially from elongation because physical processes rather than biological activities produce stretching. The axis of displacement of the hexagons varies irregularly within the same mesh, and groups of stretched hexagons are located close to those that are not stretched. Stretching was observed in four large *Paleodictyon* specimens (*P. hexagonum*), six medium-sized (*P. majus*) and four small-sized ones (*P. latum* and *P. minimum*). In the larger forms, the major axis of the hexagons tripled in length, from 8–10 mm to 24–30 mm (Fig. 2B). Here, the stretching is usually oriented in the same direction and some rows of cells are stretched more than others (Figs. 2B, 3A, 4). Stretching also affects the shafts of large *P.* (*Ramodictyon*) *hexagonum*. Cross-section shafts may triple in length (up to 14 mm in 5 specimens; see Fig. 3A). Shafts elongate following a unidirectional alignment that forms an angle ≤90° with the main stretching orientation of *Glenodictyum* mesh (see white arrows of Str in Figs. 3A–B). Radiating and grouped elements of knob-shaped *Lorenzinia* and *Parahaentzschelinia* were stretched, and smoothed structures occurred (Figs. 3B–E; 6E, *Ramodictyon* shafts). Stretching is rare in ramous-shaped *Desmograpton* (Figs. 3F, H) and *Urohelminthoida* and mainly involves longitudinal bars. Some stretched hexagons show thickened parts; in this case thickening occurs unidirectionally producing horseshoe-shaped structures in some specimens of *Paleodictyon majus*. These may have been related to an increased volume of particles due to the physical action of a current (Fig. 2E). Thickening, therefore, caused by physical action should be considered separately from the same effect produced by a biogenic action, even though only one type is shown in Figure 4. In *Paleodictyon majus* (Fig. 2E) and in another specimen of *Urohelminthoida dertonensis* (Fig. 3H; see the thick-branched meander enlarged in the oval), thickening seems to indicate a superimposion of biogenic activity (Figs. 2E, 3H), which was probably induced by burrowing meiofauna (Bromley, 1996).

Tapering.—Tapering (Tpr) has rarely been observed; it mainly affects knobs and shafts as well as the mesh hexagons of large- to medium-sized *Paleodictyon* specimens (Fig. 3A). Knobs and cells changed their shape to subtrapezoidal. Bending and tapering have been observed as two different effects of the same fluting process(es) produced by currents (Fig. 3A), and some parts of the studied burrows were selectively affected (Fig. 4). Tapered and bent segments usually end in smoothed structures (Figs. 3A, 4), which are unidirectional and iso-oriented and form a 50°–80° angle with the main stretching axis. This suggests an interaction with the current flow at the water-sediment interface (see directions of Bnd, Tpr, and Smo with respect to those of Str in Fig. 3A).

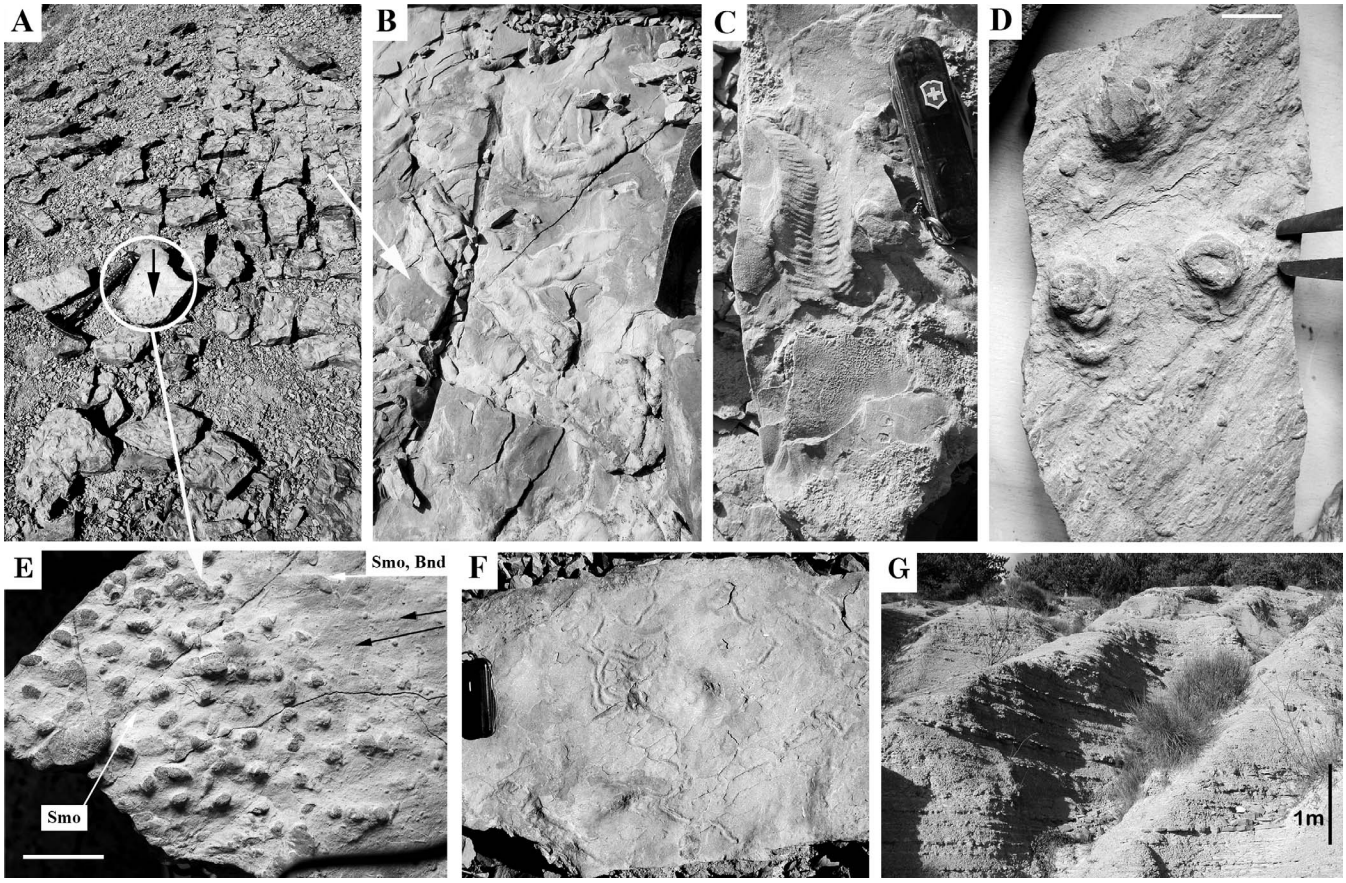

FIGURE 6—Hypichnial graphoglyptids and epichnial traces developed in thin-bedded turbidites of deep-sea fringe deposits in the Verghereto High, Verghereto Formation, Miocene. A) Top of thin-bedded turbidite shows post-depositional trace fossils; endichnia are those represented in B and C; in the circle; note the turned-out sample exhibiting the sole with shafts of *Paleodictyon* (*Ramodictyon*) *hexagonum*; hammer for scale. B) Detail of rippled top of bed with *Scolicia prisca* trails; hammer for scale. C) Detail of same bed with *Scolicia* cf. *vertebralis*; knife is 6 cm long. D) Sole of same bed with *Bergaueria*? and *Desmograpton*; bar is 1 cm. E) Detail of bent (Bnd) and smoothed (Smo) shafts of *P.* (*R.*) *hexagonum* at sole of thin-bedded turbidite; note mud-current lineations MCL (black arrows); bar is 2 cm. F) Top of bioturbated bed by *Nereites* isp.; Balze of Verghereto; knife is 6 cm long. G) General view of centimeter thin-bedded turbidites forming fringe deposits in the southern side of Verghereto High; bar is 1 m long.

Thinning.—Thinning (Thn), the decrease in string width, has been observed in partially preserved meshes, and string width may be reduced by one-half (Fig. 4). This feature has been observed in *P. majus* and *P. minimum* and may be produced by stretching (Figs. 3C–D). In fact, plastic deformation of a stretched structure will result in a thinning perpendicular to the direction of stretching.

Straightening.—Straightening (Stg), the final unusual type of deformation, was observed in two small species of *Paleodictyon* (*P. minimum*, Figs. 3C–C1, and *P. latum*), whereas it is less developed in *P. majus*. This type of deformation is observed when lateral tunnels of cells are oriented along lines parallel to the main current flow direction; the string diameter of the lateral walls is also subject to thinning (Fig. 3C–D). Straightening is hard to interpret because the studied material cannot be examined in detail due to the poor preservation of some samples (Fig. 4). In many specimens, straightening and thinning only affect some parts of a mesh (Fig. 3C1), and other parts remain intact and are not deformed (Fig. 3C1). These features also affect many minute graphoglyptids distributed throughout the same level.

DISCUSSION

The complete geometry of the graphoglyptids cannot be easily determined due to the paucity of information about their structures in deep-sea systems. Some are horizontal, as in *Paleodictyon* meshes, whereas others are helicoidal, twisted, or radiated forms developed in a complex 3-D method (see figures in Seilacher, 1977b; Uchman 1995a and references therein). Some forms disappear from the bedding plane and intrude in the muddy sediment or vice versa (e.g., *Protovirgularia vagans*), becoming endichnia and related variants (see also Monaco and Caracuel, 2007; Monaco et al., 2007). This phenomenon could be due to irregularities in the seafloor, but the variation in the orientation of the traces that enter the sediment from the surface could also be a response to food distribution and to changes in various geochemical parameters. This was observed in *Protovirgularia* and in other cases of predepositional string-shaped burrows (e.g., *Spongeliomorpha*). These traces often changed from horizontal to oblique by intruding into the mud and displacing pre-existing physical and biological structures (Fig. 7). This kind of change in geometry is less common for graphoglyptids.

Differential compaction was another problem in the taphonomic study because it could affect trace preservation and influence the observable taphonomic features. Caracuel et al. (2000) discussed this issue regarding the Early Jurassic Ammonitico Rosso facies. The compaction of some trace fossils, mainly endichnia, in those deposits varied depending on the lithology. In some instances, the tunnel cross sections were nearly circular, whereas in other cases they were elliptical. Intermediate shapes were also observed. These findings suggest that the trace fossils underwent a progressive flattening due to a compaction that was perpendicular to the stratification (Caracuel et al., 2000). After analyzing several samples, Caracuel et al. (2000) defined decompaction numbers (nd), whose

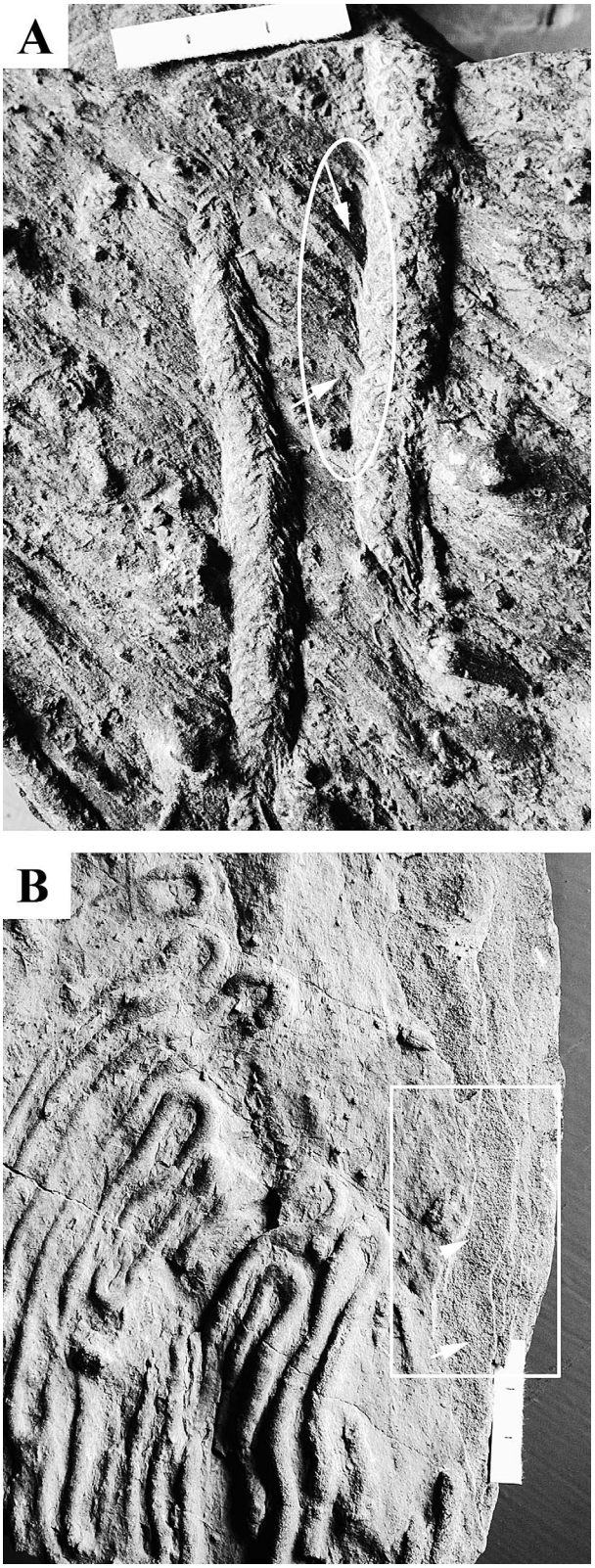

FIGURE 7—Trace fossils; bar = 3 cm. A) Intrusion of string-shaped burrows (*Protovirgularia*?) through pre-existing mud-current lineations produced hooked structures, oriented in the direction of the intrusion (arrows in oval); Verghereto Formation (Montecoronaro). B) Nearly complete absence of mica flakes at the sole of thin-bedded turbidite (hypichnial level of *Helminthorhaphe*, left side); mica very abundant in the overlying laminae (arrows in rectangle); Cervarola Formation (Monte Filetto).

values depend on the lithology: higher values were assigned to clayey marl levels (nd = 2.5), intermediate values for marls (nd = 1.67), and lower values for limestones or marly limestones (nd = 1.43) and calcarenites (nd = 1.10). In the case of graphoglyptids, deformation due to differential compaction of the predepositional traces formed on mud is certainly possible because it was probably of a greater magnitude than that of the overhanging calcarenite bed. In some thick levels (e.g., high-density turbidites), such taphonomic features of predepositional graphoglyptids as widening, tapering, and perhaps bending could have been enhanced by mass deposition of the sandy turbidite material. Bending and tapering are always orthogonal to the direction of maximum compaction and are iso-oriented with the smoothing and mud-current lineations. This suggests that the vertical compaction processes had less effect than the horizontal current-induced deformations. Furthermore, widening was never associated with bending or tapering, whereas flattened branching points were found in the same mesh level very close to other thickened parts associated with microbioturbation.

Differential compaction is also a process that acts on a single level. Sand filling in tubes surrounded by mud could surely cause differential lateral deformation, as the degree of compaction in the sand is less than that in the surrounding mud. This process enlarged and flattened the branching points of the meshes, or produced other complex deformations in samples that displayed anomalous thickening and widening. The constant presence of undeformed microbioturbation within or around the thickened areas, however, suggests that this localized compaction was either subordinate or complementary (see Knaust, 2007). Although the diagenetic evolution of the system in this location has not been adequately studied, various kinds of differential compaction can be distinguished, based on reasons presented here. These processes are negligible or circumscribed in relation to the physical action of the currents.

To explain the taphonomic characteristics of *Paleodictyon* specimens as well as other graphoglyptids and nongraphoglyptid trace fossils, a synthetic three-step model is proposed (Fig. 5): (1) predepositional burrowing; (2) biostratinomic features (B1 biogenic and B2 physical) affecting hollow shaft, knobs, meshes, and ramous meanders; and (3) initial filling and burial of turbidite sand.

Predepositional Burrowing.—In the preturbiditic stage, tunnel systems were produced in a muddy seafloor, forming nets of hexagonal meshes and vertical shafts, or plug-shaped, meander-shaped or string-shaped burrows (Fig. 5A). *Paleodictyon* nets and shafts have been found in modern deep-sea sediment and in box cores from the Mid-Atlantic Ridge. Few studies have been conducted on the organisms that produced these traces so their identity is uncertain (Rona and Merrill, 1978; Ekdale, 1980; Rona et al., 2003; Seilacher, 2007). Swinbanks (1982) suggested that infaunal xenophyophores—giant protozoans that can produce branching, polygonal meshes in poorly sorted sandy mud fill—may have been the leading producers of geometrical networks (mainly *Occultammina*, Levin, 1994). As observed in modern seafloors (Gaillard, 1991), the main mesh level lies horizontally in the mud and is exposed on the seafloor, usually 2–4 cm below the sediment-water surface, whereas shafts which connect meshes to the sea-floor surface are mostly vertical (see IMAX movie, Low, 2003). The 2–4 cm difference in height (the step in Figs. 3A–B, 5B1) has also been observed in samples from the Apennines. The step between the deep mesh level (*Glenodictyum*) and the surface shaft level (*Ramodictyon*) is the erosional gap between the two levels. The step allows the original flow characteristics to be recognized. Where the flow was stronger and eroded more, the mesh level was reached and was exposed to taphonomic action. Only the shafts were exposed and preserved with their typical elongation where the flow was weaker (Elg in Fig. 5A). This step can be considered a diagenetic ''freezing'' of multilayer erosion.

As observed in this study, other mesh levels can develop and likely indicate that there are different strategies for utilizing the seafloor deposits. Multilevel burrowing has been observed in large and small *Paleodictyon* specimens; this suggests that there are similar strategies for exploiting the muddy seafloor (Fig. 5A). Deep levels could be used to

find a more stable tier within the seafloor or for farming bacteria at lower levels. In contrast, shallow levels could be the site of new activity of tracemakers keeping pace with sediment accretion, or reflect the need to colonize a shallow horizon in order to oxygenate the burrow systems (see 2Msh in Fig. 5A).

Biostratinomic Features.—Prior to the final burial, the late phase consists of biogenic and physical processes (see Fig. 5B1 and 5B2, respectively) that affect meshes, knobs, meanders and strings. It may take place in the mud, thereby producing typical biostratinomic features as bulldozing, which is the most important surface feature. As usually defined, bulldozing only takes place near the surface or in the shallowest levels and induces 3-D deformation (twisting, squeezing, tilting, and thickening). Corresponding processes that take place in deeper levels (burrowing) cause similar mesh deformation (Fig. 5B1). The intruding action in the mud is very common. The string-shaped trace fossils *Spongeliomorpha* and *Protovirgularia* bend and displace the pre-existing structures in several studied specimens. In one instance, an intrusion between the meanders of a *Desmograpton* forms opposite rows of meanders that are about 2 cm from each another.

Such benthic community members as irregular echinoids, crustaceans, teleost fishes, polychaetes and many other soft-body organisms can produce bulldozing and burrowing in many types of marine media (substrates) that comprise the seafloor (Seilacher, 1974; 2007; Frey and Pemberton, 1984; Ekdale, 1985; Kidwell, 1991; Goldring, 1995; Kanazawa, 1995; Bromley, 1996; Monaco et al., 2005). Few direct observations have investigated the benthic behavior in deep-sea muddy environments (Rona and Merrill, 1978; Gaillard, 1991; Rona, 2004). Biogenic deformation can be produced by the burrowing of crustacean decapods or irregular echinoids; they deform the sediment while moving through it. This kind of activity squeezes many particles (Kanazawa, 1995; Monaco et al., 2005) and may affect graphoglyptids. Microburrowing of meiofauna is another common process that produces thickening and widening in mesh walls and may involve many parts of the burrow (Fig. 5B1). This process can also be generated by a microbioturbating community and may be related to the activity of microorganisms (Yingst and Rhoads, 1980; Knaust, 2007). Microbioturbation also is found inside open, uninhabited graphoglyptid mesh. This suggests that elongated or enlarged portions of many burrows (Figs. 2D, 5B1) were ideal zones in which microtracemakers were able to exploit microbial growth, organic matter, and bacteria concentrations (amensalism relationships, see Levinton, 1977).

Physical processes are those caused by the effects of currents that induced unidirectional deformations (stretching, straightening, smoothing, thickening, bending, tapering, and thinning; see Fig. 5B2). These characteristics are associated with abundant microstructures induced by currents, namely minigrooves, which developed in interturbidite deposits. Minigrooves are straight, horizontal lineations, 10–30 mm in length and 0.2–0.8 mm thick. They are arranged in groups of 5–10 per square decimeter and are distributed parallel to many biostratinomic features. They can also be defined as mud-current lineations (Figs. 3C, G, 5B2). They are oriented similarly to the straight lines of the hexagons of *Paleodictyon minimum* and *P. latum* or the smoothed semirelief of *Helminthorhaphe*. They were probably formed at the sediment-water interface, which would suggest bottom-current interference on the seafloor (Figs. 3C, G, 5B2). In some instances, the intrusion of string-shaped burrows (*Protovirgularia*?) through the pre-existing mud-current lineations produced hooked structures, oriented in the direction of the intrusion itself (Fig. 7A). This implies that the intrusion took place after the current structures were produced on stiff mud. These microstructures remained intact in the final fine-grained sand burial. The orientation of mud-current lineations may reflect the activity of preturbidite currents. Preturbidite flows, while still poorly understood, probably influenced *Paleodictyon* net orientation and elongation, as proposed for the Silurian of Wales (interturbidite flows) by Crimes and Crossley (1980). Preturbidite current flows in the studied deposits are distributed at angles from 0° to 80° with respect to the main turbidite current indicators (cm- to dm-scale groove and flute casts), which are aligned NW–SE, following the main foredeep depocenters of the Apennines (Ricci-Lucchi, 1981). Due to the extreme complexity of the Apennine foredeep basin seafloor, however, this angular divergence cannot be used as a safe indicator of the paleodepositional setting.

Erosional processes probably occurred in the mud, thereby eroding some layers to expose the deepest mesh levels. In the case of *Paleodictyon minimum* and *P. latum*, erosion only affects the seafloor to a depth of a few millimeters in the distal part of the basins, whereas it reaches a few centimeters in the depositional lobes in the case of *P. hexagonum*. In the phase of preturbidite current flows, burrow parts are elongated with their major axis parallel to the current indicators. In fluted semireliefs of the graphoglyptids (see Seilacher, 1977b; Crimes and Crossley, 1980), tunnel reinforcement by mucus film seems to have preserved the outer lining of the walls from erosion and filling. Fluting processes, however, demonstrate that some parts may have been destroyed by the current (e.g., smoothing), whereas others remained undisturbed (Figs. 3G, 5B2).

Large *Paleodictyon* specimens (e.g., *P. hexagonum*) are instructive because the shafts doubled in length by stretching, but deformed mesh hexagons are three to four times larger than the undeformed ones (8–10 mm and 24–33 mm long for each hexagon, respectively). Moreover, the deformation of the hexagons is very irregular and many parts of the net are deformed or stretched and have different lengths and thicknesses (Fig. 2A, H). Differential stretching and deformation seems to indicate that a linear current selectively involved some portions of the burrow system on the seafloor. In steep slope areas, there may have been other causes than simple current effects. Analysis of the mesh deformations in large *Paleodictyon* specimens coming from slopes suggests that these features were produced directly in the mud and may have been influenced by creep (Fig. 5B2), since there is some evidence of mass movements involving different beds. Creep affects poorly consolidated mud and can produce an irregular deformation (mainly unidirectional) in the down-dip direction of the slope. In these areas, some thin fractures are often orthogonal to the predominant elongation and were probably produced during the strain related to the creeping of mud. The incline of the slope and the very poor consolidation of the mud would stretch the soft material. Unidirectional downslope-oriented currents may have enhanced this feature (Fig. 5B2). Markedly stretched *P. hexagonum* specimens are very common on the sloping sides of isolated submarine highs and ridges. These frequent seafloor irregularities (e.g., southwestern slope of the Verghereto High, Canili) are due to compressive tectonics in the Apennine foredeep. In the dipping areas current-induced phenomena co-existed locally with creeping.

Organisms that produced large *P. hexagonum* were probably well adapted to life in sloped areas, where longitudinal to transverse-oriented bottom currents were active (Crimes and Crossley, 1980). In these areas, bulldozing, burrowing, and slope instability destroyed and deformed parts of the mesh. When the organisms tried to repair their work, they produced another mesh at a different, more stable level. In fact, as can be seen in many large specimens, some levels of meshes are superimposed and translated by 10–20 mm. This suggests that there was a biogenic response to burrow destruction or seafloor instability (Fig. 2G). Where creep is lacking, as in some stable areas of the basin plain subenvironments where fine-grained, regular, thin beds are found, such small *Paleodictyon* species as *P. strozzii*, *P. majus*, *P. italicum*, *P. latum*, and *Paleodictyon* isp. lengthened their cells equidimensionally and their action reflects the response of the tracemaker(s) to the currents.

Final Stage, Initial Filling and Burial by Thin-bedded Turbidite Material.—The final stage consists of a progressive deposition of fine material with two different phases: an initial slow filling and a subsequent burial by thin-bedded turbidite deposit (Figs. 5C1–2). The initial filling slowly coated the graphoglyptids and all predepositional taphonomic features to form a thin layer, 0.5–1.0 mm thick, of fine grains (carbonate silt and fine sand), in which mica was virtually absent. The initial filling is here indicated as the fine spread level; it sticks to biogenic mucus film and preserves all delicate structures (FSL in Fig. 5C1). The preservation

of all the microstructures, including complete 0.06 mm nets, suggests that the fine spread level must have formed progressively and delicately. It may have acted like a gluey film trapping fine particles settled from the suspension on the seafloor; an early cementation occurred creating a thin firm level that glued to the micaceous-rich material of the turbidite. The high carbonate content in the basal level indicates that it must have been affected by early consolidation and had hardened before the first phases of turbidite deposition. This early cementing film could explain the perfect preservation of the microstructures, even though diluted turbiditic flows were deposited subsequently. This process may show some similarities with the penecontemporaneous partially lithified crust (PPLC) described by Woodmorappe (2006), but it needs to be investigated further given the new field data and specific laboratory analyses (e.g., geochemistry). Similarly, virtual absence of mica flakes in the basal film, which is very abundant in all the overlying laminae (see Fig. 7B), could be the result of a different type of flow with different composition, or micaceous elements may not have been preserved. This issue needs further petrographic investigations. No erosion or further compaction took place during this phase, and all of the microstructures in the interturbidite mud, such as mud-current lineations, mesh elongations (straight striae), and other taphonomic features of phase B have been preserved. Where such small *Paleodictyon* species as *P. minimum*, *P. strozzii*, *P. majus*, *P. italicum*, *P. latum*, and *Paleodictyon* isp. and other delicate graphoglyptids are preserved, the fine spread level can be observed as thin-cemented film in a side view.

The second phase is the subsequent deposition of thin-bedded material from low-density turbidite flows (Fig. 5C2). The material consists of many thin laminae, 0.5–1 mm thick, that are very rich in mica flakes (Fig. 7B, arrows). Micaceous sandy laminae may have been formed by the settling from suspension followed by thin laminar flows from the diluted flows. Deposits may correspond to the distal facies F9a and F9b of the low-density turbidity currents (Mutti, 1992), which are partially compatible with the upper divisions of the Bouma sequence. The erosive potential of such a turbidity flow is insignificant, and a settling from suspension occurs in the distal areas. According to Pickering et al. (1989) and Mutti (1992), laminar flows progressively turn into turbulent ones in more distal areas, and their erosive potential on the seafloor decreases progressively. Typical erosion may have been limited to the bypass areas (see scoured surfaces in Uchman, 1995a, pl. 15, fig. 5) and was induced by traction carpets and tractive flows. When traction carpets (i.e., F7 and other proximal facies) developed, the turbidite soles are devoid of any graphoglyptids but are rich in *Scolicia strozzii* and *Ophiomorpha* isp., which are typical post-depositional trace fossils of high-energy regimes (Tunis and Uchman, 1996a, 1996b; Uchman, 1999; Wetzel and Uchman, 2001; Uchman et al., 2004).

Trace fossil communities are also typically found in the top of the turbidite beds. In some *Paleodictyon*-bearing beds, current ripples are found in facies F9b (e.g., Verghereto fringing deposits). Here the bed sequence starts and ends with ripples, which are orthogonal to the main turbidity flows. It can be inferred that bottom currents persisted and it is crucial to understand the facies development, as indicated in many basin analyses (Crimes and Crossley, 1980; Pickering et al., 1989; Mutti, 1992; Rebesco and Viana, 2005). The silty to muddy, rippled, topmost surface usually has a very rich trace-fossil community totally different from the predepositional graphoglyptid assemblage (Figs. 6A–G). This top community (e.g., Montecoronaro of Verghereto) is usually characteristic of the 3–6-cm-thick, thin-bedded turbidite beds (see Fig. 6G) and the predominant post-depositional trace fossils are *Scolicia prisca*, *S. vertebralis* (cf. Uchman, 1998, fig. 58b), *Nereites missouriensis*, and other epichnial forms (Figs. 6B–C, F). These post-depositional trace fossils were produced by opportunistic organisms (mainly irregular echinoids) under specific seafloor conditions (see sequential colonization of Wetzel and Uchman, 2001; and tiering pattern of Uchman, 1995b). There was competition to exploit the organic matter and abundant food deposited by turbidite settling (Figs. 6A–E). The *Scolicia prisca* ichnoassemblage is well exposed in a 50-m^2 area in the Montecoronaro outcrop where densely packed trails of 100 specimens/m^2 have been recorded (Figs. 6A–C).

CONCLUSIONS

This study is an attempt to understand the widespread graphoglyptid preservation patterns in turbidite systems. The conclusions discussed below can be considered hypotheses that require additional analysis and testing of their facies distribution based on the data gathered from other flysch deposits of the northern Apennines and from deposits of different ages and locations.

Graphoglyptids and associated hypichnial trace fossils are crucial for turbidite analysis; they are abundant and well preserved in some beds (e.g., fine-grained deposits). Taphonomic features of meshes, shafts, knobs, meanders, and strings may be quantified by observing the changes in their geometric patterns. Biogenic and physical taphonomic features are particularly important because some of these are typical of large specimens (e.g., stretching), whereas others are characteristic of smaller ones (e.g., elongation). Certain characteristics can also be recognized at different depths below the seafloor (i.e., two different meshes for many *Paleodictyon* specimens). Some of the features suggest that biogenic 3-D deformation—mainly twisting, squeezing, tilting, and thickening—are often controlled and enhanced unidirectionally by such physical agents as currents. This is demonstrated by elongation, which supports the hypothesis of Crimes and Crossley (1980). These currents cause other such fluting deformations as bending, tapering, straightening, and smoothing. Bottom instability (e.g., creep) is another factor that influences deformation in the slope areas, which are irregularly distributed following the complexity of the Apennine foredeep basins. In some thin-bedded turbidites (i.e., fringing deposits of the Montecoronaro–Verghereto High), both biogenic- and physically induced taphonomic characteristics of hypichnial and epichnial communities can be compared.

Deep-sea sedimentologists and ichnologists have explained the preservation of graphoglyptids and other hypichnia at the soles of turbidites in a rather dogmatic way, but a truly convincing model for taphonomic alterations has never been proposed. Two hypotheses are proposed in relation to two different types of currents.

The first relates to long-term current action prior to a turbidite flow (interturbiditic bottom currents). To validate this hypothesis–that contour currents precede (even for a long time) the turbiditic filling—many regional studies of the interturbidite mud and tool marks at the sole of turbidites are needed. Paleocurrents that are orthogonal or that clearly diverge from the main turbiditic flows should be examined. While this aspect was presented in the model of Crimes and Crossley (1980), an orthogonal dispersion of currents was never observed in the present study. Proof of the existence of an unambiguous causal relationship between the taphonomic characteristics of the ichnotaxa (see elongation) and the action of interturbiditic currents would be of great importance. Such proof is difficult to demonstrate, especially in such an articulated foredeep like that of the Apennine. Detailed geological analyses, geochemical studies, and comparisons of predepositional structures in interturbidite mud are needed. Preservation of delicate variations in graphoglyptid shape and mud-current lineations implies that the erosive potential of turbidite flows, described in the literature, has been overestimated and difficult to appraise. In contrast, the bottom-current activity that affects the interturbidite mud is poorly understood and may be underestimated.

The second hypothesis relates to current action prior to and during the turbiditic flow (many models). This idea implies that the paleocurrent indicators are arranged in the same direction as the main turbiditic flow, or may vary by a few degrees due to flow interference. To validate this hypothesis, it would be important to demonstrate that flows were selective and so delicate that they preserved all features and produced only minimal deformation of the graphoglyptids. Flows twisted the burrows, but did not erode them; they stretched hexagons but preserved minute structures, up to 0.06 mm thick. Generally speaking, this scenario does not fit

a classic turbiditic deposition *sensu stricto*, where the instant acceleration of turbid water body in front of turbidite sand may produce a shock wave with a sucking of the unconsolidated surface mud into suspension (Seilacher, 2007, p. 150); it is difficult to find these aspects in very fine-grained turbidites and very low-density flows. One can only imagine a distal-flow of a laminar water mass, which preceded the sand of the turbiditic body but was strictly associated with it. This laminar water acted on the sea-bottom mud, deforming the burrows (possibly immediately) before the final burial of sand transported by the turbiditic flow itself. In any case, the initial filling with fine material had to be gentle and completely nondestructive. The initial filling may not have been related to the laminar action of a distal turbiditic flow, but rather could have been due to a settling process that occurred before the flow itself. This settling would have produced a thin layer involved in early diagenesis; it probably hardened before the arrival of the turbiditic flows. The mud-current lineations, as well as the taphonomic features would have been perfectly preserved.

While the trace fossils examined in this study do not provide enough evidence to select one of the two hypotheses, neither can be ruled out. The taphonomic methodology applied to the graphoglyptids and hypichnia trace fossils is extremely promising and will be further developed in future studies.

ACKNOWLEDGMENTS

Field work was carried out with the help of M. Gabrielli, M. Quirini, M. Milighetti, and T. Trecci. I am very grateful to A. Uchman and to an anonymous reviewer for useful and detailed suggestions for improving the manuscript, and to S.T. Hasiotis, coeditor of PALAIOS, for his useful suggestions. I am also grateful to M. Rebesco and D. Stow for stimulating discussions on seafloor bottom currents at the GeoItalia 2005 forum at Spoleto, Italy. Many thanks to M. Bilotta and R. Rinaldi for their editorial and linguistic assistance. This research was supported by research project RB 2006–2007 of the Earth Science Department of the University of Perugia.

REFERENCES

Abbate, E., and Bruni, P., 1989, Modino-Cervarola o Modino e Cervarola? Torbiditi oligo-mioceniche ed evoluzione del margine nord-Appenninico: Memorie Società Geologica Italiana, v. 6(1987), p. 19–33.

Boccaletti, M., and Coli, M., eds., 1982, Carta Strutturale dell'Appennino Settentrionale, 1:250.000: Selca, Firenze.

Boccaletti, M., Calamita, F., Deiana, G., Gelati, R., Massari, F., Moratti, G., and Ricci Lucchi, F., 1990, Migrating foredeep-thrust belt system in the northern Apennines and southern Alps: Palaeogeography, Palaeoclimatology, Palaeoecology, v. 77, p. 3–14.

Bromley, R.G., 1990, Trace Fossils, Biology and Taphonomy: Unwin Hyman Ltd., London, 280 p.

Bromley, R.G., 1996, Trace Fossils, Biology, Taphonomy and Application: Chapman & Hall, London, 361 p.

Caracuel, J.E., Monaco, P., and Olóriz, F., 2000, Taphonomic tools to evaluate sedimentation rates and stratigraphic completeness in Rosso Ammonitico facies (epioceanic tethyan Jurassic): Rivista Italiana Paleontologia e Stratigrafia, Milan, v. 106(3), p. 353–368.

Caracuel, J.E., Giannetti, A., and Monaco, P., 2005, Multivariate analysis of taphonomic data in Lower Jurassic carbonate platform (northern Italy): Compte Rendue Palevol (2005), v. 4, p. 653–662.

Costa, E., Giulio, A.D., Plesi, G., Villa, G., and Baldini, C., 1997, I flysch oligomiocenici della trasversale toscana meridionale-Casentino: Dati biostratigrafici e petrografici: Atti Ticinensi Scienze Terra, v. 39, p. 281–302.

Crimes, T.P., and Crossley, J.D., 1980, Inter-turbidite bottom current orientation from trace fossils with an example from the Silurian flysch of Wales: Journal of Sedimentary Petrology, Tulsa, v. 50, p. 821–830.

Ekdale, A.A., 1980, Graphoglyptid burrows in modern deep-sea sediments: Science, v. 207, p. 304–306.

Ekdale, A.A., 1985, Paleoecology of the marine endobenthos: Palaeogeography, Palaeoclimatology, Palaeoecology, v. 50, p. 63–81.

Fernández López, S., 1997, Ammonites, taphonomic cycles and stratigraphic cycles in carbonate epicontinental platforms: Cuadernos de Geología Ibérica, v. 23, p. 95–136.

Frey, R.W., and Pemberton, S.G., 1984, Trace fossil facies models, *in* Walker, R.G., ed., Facies Models, Geoscience Canada Reprint Series, 2nd ed., Calgary, p. 189–207.

Fuchs, T., 1895, Studien über Fucoiden und Hieroglyphen: Denkschriften der Kaiserlichen Akademie der Wissenschaften, Wien, Mathematisch-Naturwissenschaftliche, Klasse, v. 62, p. 369–448.

Gaillard, C., 1991, Recent organism traces and ichnofacies on the deep-sea floor of New Caledonia, southwestern Pacific: Palaios, v. 6, p. 302–315.

Goldring, R., 1995, Organisms and the substrate: Response and effect, *in* Bosence, D.W.J., and Allison, P.A., eds., Marine Palaeoenvironmental Analysis from Fossils: Geological Society, London, Special Publication no. 83, p. 151–180.

Honeycutt, C.E., and Plotnick, R.E., 2005, Mathematical analysis of *Paleodictyon*: A graph theory approach: Lethaia, v. 38(4), p. 345–350.

Kanazawa, K., 1995, How spatangoids produce their traces: Relationship between burrowing mechanism and trace structure: Lethaia, v. 28, p. 211–219.

Kidwell, S.M., 1991, Taphonomic feedback (live/dead interactions) in the genesis of bioclastic beds: Keys to reconstructing sedimentary dynamics, *in* Einsele, G., Ricken, W., and Seilacher, A., eds., Cycles and Events in Stratigraphy: Springer Verlag, Berlin, Heidelberg, New York, p. 268–282.

Knaust, D., 2007, Meiobenthic trace fossils as keys to the taphonomic history of shallow-marine epicontinental carbonates, *in* Miller III, W., ed., Trace Fossils: Concepts, Problems, Prospects: Elsevier, Arcata, California, p. 502–517.

Koriba, K., and Miki, S., 1939, On *Paleodictyon* and fossil *Hydrodictyon*: Jubilee Publication in the Commemoration of Prof. H. Yabe, M.I.A.16th Birthday, Tohoku University, v. 1, p. 55–61.

Książkiewicz, M., 1954, Uziarnienie frakcjonalne i laminowane we fliszu karpackim (Graded and laminated bedding in the Carpathian Flysch): Rocznik Polskiego Towarzystwa Geologicznego, v. 22, p. 399–471.

Książkiewicz, M., 1970, Observations on the ichnofauna of the Polish Carpathians, *in* Crimes, T.P., and Harper, J.C., eds., Trace Fossils, Geological Journal Special Issue, Liverpool, p. 283–322.

Książkiewicz, M., 1977, Trace fossils in the flysch of the Polish Carpathians: Paleontologica Polonica, v. 36, p. 1–208.

Levin, L.A., 1994, Paleoecology and ecology of Xenophyophores: Palaios, v. 9, p. 32–41.

Levinton, J.S., 1977, Ecology of shallow water deposit-feeding communities, Quisset Harbor, Massachussets, *in* Coull, B.C., ed., Ecology of Marine Benthos: University of South Carolina Press, Columbia, p. 191–227.

Low, S., 2003, Volcanoes of the deep sea: IMAX movie produced by University Relations for Faculty and Staff of Rutgers, State University of New Jersey, by NSF, http://www.volcanoesofthedeepsea.com/. Checked May 2005.

Menghini, G.G., 1850, Osservazioni stratigrafiche e paleontologiche concernenti la geologia della Toscana e dei paesi limitrofi, *in* Murchison, R.I., ed., Memoria sulla Struttura Geologica delle Alpi, degli Appennini e dei Carpazi: Stamperia Granducale, Firenze, p. 246–528.

Miller, W., III, 1991, Paleoecology of graphoglyptids: Ichnos, v. 1, p. 305–312.

Monaco, P., 2000, Biological and physical agents of shell concentrations of *Lithiotis* facies enhanced by microstratigraphy and taphonomy, Early Jurassic, Gray Limestones Formation, Trento area (Northern Italy), *in* Hall, R., and Smith, P., eds., Advances in Jurassic Research 2000, Proceedings of the 5th International Symposium on the Jurassic System, Vancouver B.C. (Canada), August 12–25, 1998: GeoResearch Forum, Trans Tech, Basel, p. 473–486.

Monaco, P., and Caracuel, J.E., 2007, Il valore stratinomico delle tracce fossili negli strato evento (event bed) del registro geologico: esempi significativi di ichnologia comportamentale dall'Italia e dalla Spagna: Studi e Ricerche, Museo ''G. Zannato'' Montecchio Maggiore (VI), v. 14, p. 43–61.

Monaco, P., Caracuel, J.E., Giannetti, A., Soria, J.M., and Yébenes, A., 2007, *Thalassinoides* and *Ophiomorpha* as cross-facies trace fossils of crustaceans from shallow to deep-water environments: Mesozoic and Tertiary examples from Italy and Spain, *in* Garassino, A., Feldmann, R. M, and Teruzzi, G., eds., 3rd Symposium on Mesozoic and Cenozoic Decapod Crustaceans: Memorie Società Italiana Scienze Naturali e Museo Civico Storia Naturale Milano, May 23–25, 2007, p. 79–82.

Monaco, P., and Giannetti, A., 2002, Three-dimensional burrow systems and taphofacies in shallowing-upward parasequences, lower Jurassic carbonate platform (Calcari Grigi, Southern Alps, Italy): Facies, v. 47, p. 57–82.

Monaco, P., Giannetti, A., Caracuel, J.E., and Yébenes, A., 2005, Lower Cretaceous (Albian) shell-armoured and associated echinoid trace fossils from the Sácaras Formation, Serra Gelada area, southeast Spain: Lethaia, v. 38, p. 1–13.

Monaco, P., and Uchman, A., 1999, Deep-sea ichnoassemblages and ichnofabrics of the Eocene Scisti varicolori beds in the Trasimeno area, western Umbria, Italy, *in* Farinacci, A., and Lord, A.R., eds., Depositional Episodes and Bioevents: Paleopelagos, Università La Sapienza, Special Publication No. 2, Roma, p. 39–52.

Mutti, E., 1992, Turbidite Sandstone: AGIP S. p.a., San Donato Milanese, 275 p.

Mutti, E., and Normark, W.R., 1987, Comparing examples of modern and ancient turbidite systems: Problems and Concepts, *in* Legget, J.K., and Zuffa, G.G., eds.,

Marine Clastic Sedimentology: Concepts and Case Studied: Graham & Trotman, p. 1–38.

Orr, P.J., 2001, Colonization of the deep-marine environment during the Early Phanerozoic: The ichnofaunal record: Geological Journal, v. 36, p. 265–278.

Peruzzi, D.G., 1881, Osservazioni sui generi *Paleodictyon* e *Paleomeandron* dei terreni Cretacei ed Eocenici dell'Appennino Settentrionale e Centrale: Atti Società Toscana Scienze Naturali Memorie, v. 5(1), p. 3–8, Pisa.

Pickering, K.T., Hiscott, R.N., and Hein, F.J., 1989, Deep Marine Environments: Clastic Sedimentation and Tectonics: Unwin Hyman Ltd., London, 416 p.

Piper, D.J.W., and Stow, D.A.V., 1991, Fine-grained turbidites, *in* Einsele, G., Ricken, W., and Seilacher, A., eds., Cycles and Events in Stratigraphy: Springer-Verlag, Berlin, Heidelberg, p. 360–376.

Plesi, G., Luchetti, L., Boscherini, A., Botti, F., Brozzetti, F., Bucefalo Palliani, R., Daniele, G., Motti, A., Nocchi, M., and Rettori, R., 2002, The Tuscan successions of the high Tiber Valley (Foglio 289–Città di Castello): Biostratigraphic, petrographic and structural features, regional correlations: Bollettino Società Geologica Italiana, Volume speciale no. 1, p. 425–436.

Ray, A.J., and Aller, R.C., 1985, Physical irrigation of relict burrows: Implications for sediment chemistry: Marine Geology, v. 62, p. 371–379.

Rebesco, M., and Viana, A., 2005, Contourites: State-of-the-art and open questions: GeoItalia 2005, FIST, Spoleto, 21–23 Sept. 2005, 320.

Ricci-Lucchi, F., 1981, The Miocene Marnoso-Arenacea turbidites, Romagna and Umbria Apennines, *in* Ricci-Lucchi, F., ed., IAS, 2nd European Regional Meeting, Roma, Escursion Guidebook, No. 7: Tecnoprint, Bologna, p. 231–303.

Rona, P., Seilacher, A., Luginsland, H., Seilacher, E., Vargas, C.D., Vetriani, C., Bernhard, J.M., Sherrell, R.M., Grassle, J.F., Low, S., and Lutz, R.A., 2003, *Paleodictyon*, a living fossil on the Deep Sea floor: Eos Transactions AGU, Fall Meeting Supplement, Abstract OS32A-0241.

Rona, P., 2004, Secret survivor: Natural History, v. 113, p. 50–55.

Rona, P.A., and Merrill, G.F., 1978, A benthic invertebrate from the Mid-Atlantic Ridge: Bulletin Marine Science, v. 28, p. 371–375.

Sacco, F., 1888, Note di Paleoicnologia italiana: Atti Società Italiana Scienze Naturali, v. 31, p. 151–192.

Savrda, C.E., 2007, Taphonomy of Trace Fossils, *in* Miller III, W., ed., Trace Fossils: Concepts, Problems, Prospects: Elsevier, Arcata, California, p. 92–109.

Seilacher, A., 1962, Paleontological studies on turbidite sedimentation and erosion: Journal Geology, v. 70, p. 227–234.

Seilacher, A., 1974, Flysch trace fossils: Evolution of behavioural diversity in the deep-sea: Neues Jahrbuch für Geologie und Paläontologie Monatshefte, v. 4, p. 233–245.

Seilacher, A., 1977a, Evolution of trace fossil communities, *in* Hallam, A., ed., Patterns of Evolution as Illustrated by the Fossil Record, Developments in Paleontology and Stratigraphy, No.4: Elsevier, Amsterdam, p. 359–376.

Seilacher, A., 1977b, Pattern analysis of *Paleodictyon* and related Trace Fossils, *in* Crimes, T.P., and Harper, J.C., eds., Trace Fossils 2: Geological Journal, Special Issue 9, Liverpool, p. 289–334.

Seilacher, A., 2007, Trace Fossil Analysis: Springer-Verlag, Berlin, 226 p.

Stow, D.A.V., and Piper, D.J.W., eds., 1984a, Fine-grained sediments: Deep-water Processes and Facies: Geological Society, Special Publication, v. 15, 659 p.

Stow, D.A.V., and Piper, D.J.W., 1984b, Deep-water fine-grained sediments: Facies models, *in* Stow, D.A.V., and Piper, D.J.W., eds., Fine-grained sediments: Deep-water processes and facies: Geological Society, Special Publication, v. 15, p. 611–646.

Swinbanks, D.D., 1982, *Paleodictyon*: The traces of infaunal Xenophyophores?: Science, v. 218, p. 47–49.

Tunis, G., and Uchman, A., 1996a, Ichnology of Eocene Flysch deposits of the Istria Peninsula, Croatia and Slovenia: Ichnos, v. 5, p. 1–22.

Tunis, G., and Uchman, A., 1996b, Trace fossils and facies changes in Cretaceous-Eocene flysch deposits of the Julian Prealps (Italy and Slovenia): Consequences of regional and world-wide changes: Ichnos, v. 4, p. 169–190.

Uchman, A., 1995a, Taxonomy and Paleoecology of Flysch trace fossils: The Marnoso-Arenacea Formation and associated facies (Miocene, Northern Apennines, Italy): Beringeria, v. 15, 116 p.

Uchman, A., 1995b, Tiering patterns of trace fossils in the Paleogene flysch deposits of the Carpathians, Poland: Geobios, v. 18, p. 389–394.

Uchman, A., 1998, Taxonomy and ethology of flysch trace fossils: Revision of the Marian Książkiewicz collection and studies of complementary material: Annales Societatis Geologorum Poloniae, v. 68, p. 105–218.

Uchman, A., 1999, Ichnology of the Rhenodanubian Flysch (Lower Cretaceous–Eocene) in Austria and Germany: Beringeria, v. 25, p. 67–173.

Uchman, A., 2004, Phanerozoic history of deep-sea trace fossils, *in* McIlroy, D., ed., The Application of Ichnology to Palaeoenvironmental and Stratigraphic Analysis: Geological Society, Special Publication, London, p. 125–139.

Uchman, A., 2007, Deep-Sea Ichnology: Development of Major Concepts, *in* Miller III, W., ed., Trace Fossils: Concepts, Problems, Prospects: Elsevier, Arcata, California, p. 248–267.

Uchman, A., Janbu, N.E., and Nemec, W., 2004, Trace fossils in the Cretaceous–Eocene Flysch of the Sinop-Boyabat Basin, Central Pontides, Turkey: Annales Societatis Geologorum Poloniae, v. 74, p. 197–235.

Vialov, O.S., and Golev, B.T., 1965, O drobnom podrazdieleni gruppy Paleodictyonidae (in Russian only): Byulletin Moskovskovo Obshchzhestva Ispityvania Prirody, Odtiel Gieologii, v. 40, p. 93–114.

Walker, R.G., ed., 1984, Facies Models: Canada Reprints Series, Geological Association Canada, Calgary, 317 p.

Wetzel, A., 2000, Giant *Paleodictyon* in Eocene flysch: Palaeogeography, Palaeoclimatology, Palaeoecology, v. 160, p. 171–178.

Wetzel, A., and Uchman, A., 2001, Sequential colonization of muddy turbidites in the Eocene Beloveža Formation, Carpathians, Poland: Palaeogeography, Palaeoclimatology, Palaeoecology, v. 168, p. 171–186.

Woodmorappe, J., 2006, Are soft-sediment trace fossils (ichnofossils) a time problem for the Flood?, Journal of Creation, v. 20(2), p. 113–122.

Yingst, J.Y., and Rhoads, D.C., 1980, The role of bioturbation in the enhancement of bacterial growth rates in marine sediments, *in* Tenore, K.R., and Coull, B.C., eds., Marine Benthic Dynamics: University of South Carolina Press, Durham, p. 407–421.

ACCEPTED MAY 13, 2008